Gut DRP

Final Report

January 15, 1969 to May 19, 1971

EVALUATION OF ADVANCED BLADDER TECHNOLOGY

Prepared for:

JET PROPULSION LABORATORY
4800 OAK GROVE DRIVE
PASADENA, CALIFORNIA 91103

CONTRACT NAS 7-698

STANFORD RESEARCH INSTITUTE
Menlo Park, California 94025 · U.S.A.

SUMMARY

During the period of this report, January 15, 1969 to May 19, 1971, work on this project was conducted in five major categories. In four of these categories, papers have been accepted for publication.

In the first category, diffusion and permeation of CO_2, O_2, N_2, and NO_2 through polytetrafluoroethylene (PTFE) were studied. Appendix A on this subject has been published in Macromolecules. This study indicates that the gases tested, except NO_2, do not interact with the PTFE but diffuse through preexisting channels and voids.

In a second category is the study of the diffusion, permeation, and solubility of simple gases (CO_2, O_2, N_2, CH_4, C_2H_6, C_3H_8, and C_2H_4) through a copolymer of hexafluoropropylene and tetrafluoroethylene (FEP). The results of this study are summarized in Appendix B, which has been accepted for publication in Macromolecules. Existing theories of gas-polymer interactions are shown to be unable to explain satisfactorily the experimental data for FEP.

In a third category, the viscous flow and diffusion of gases through small apertures were studied. A report on this study has been accepted for publication by the Journal of Applied Physics and the manuscript appears as Appendix C. This study indicates that for the gases tested, CO_2, O_2, and N_2, the observed diffusion values are smaller than those calculated by a nearly constant factor.

A fourth category includes a study of diffusion and permeation of O_2, N_2, CO_2, CH_4, C_2H_6, and C_3H_8 through nitroso rubber. Appendix D is the manuscript of the paper, which has been accepted for publication by the Journal of Applied Polymer Science. This study shows that the solubilities of these gases in nitroso rubber are 2 to 4 times those in natural rubber. The different behavior of CO_2 indicates a strong specific interaction.

Category 5 includes the results of gas transport studies on five materials submitted by JPL. This work is summarized in the following section.

Appendix E lists other publications generated under this program or under a related NASA-JPL program.

CONTENTS

TABLES

GAS TRANSPORT STUDIES ON MATERIALS SUBMITTED TO SRI BY JPL

A. Carborane Siloxane

The sample had a very rough, grainy surface; its thickness, which was measured with a micrometer, was nominally 22 mil. Some difficulties were encountered in sealing the membrane leak-tight into the cell but they were overcome by affixing on either side of the membrane 5-mil polyethylene gaskets with RTV silicone adhesive.

The permeation and diffusion coefficients for CO_2 were determined at three temperatures. Hydrogen permeability was measured with nitrogen as carrier gas to achieve high detector sensitivity, and the detector was calibrated with a hydrogen-nitrogen mixture of known composition. After completion of the experimental series at maximum temperature (99.5°C), the membrane was badly deformed, having assumed the shape of the cell, i.e., the material had flowed.

The data for both CO_2 and H_2 are shown in Table 1. The permeation rate for hydrogen was so fast at higher temperatures that the calculated diffusion coefficients are not reliable; thus, the heat of diffusion quoted represents only a lower limit.

Table 1

PERMEATION AND DIFFUSION COEFFICIENTS OF CO_2 AND H_2 THROUGH CARBORANE SILOXANE

Permeant	Temp Range (°C)	$P_{50°} \times 10^9$ $\left(\frac{\text{cc cm}}{\text{cm}^2 \text{ sec cm Hg}}\right)$	$D_{50°} \times 10^6$ (cm^2/sec)	E_P (kcal/mole)	E_D (kcal/mole)
CO_2	48.5 - 74.9	3.9	0.50	8.4	10.5
H_2	49.2 - 99.5	5.8	1.1	7.5	> 3.7

B. Nitroso Rubber (CTVR-CTA cured batch 1254/1256)

A nitroso rubber sample 1 mm thick was studied. Table 2 lists the permeation and diffusion coefficients of CO_2 measured at five temperatures.

Table 2

PERMEATION AND DIFFUSION COEFFICIENTS OF CO_2 THROUGH A 1-mm NITROSO RUBBER MEMBRANE

t(°C)	$P \times 10^9$ $\left(\frac{cc(stp)cm}{cm^2 \text{ sec cm Hg}}\right)$	$D \times 10^7$ (cm^2/sec)
25	15.2	6.8
30	17.4	8.6
35	19.1	9.5
40	23.9	11.4
45	26.1	13.7

The heats of permeation and diffusion calculated from these data are 5.2 and 7.3 kcal/mole, respectively.

Some data on permeation through nitroso rubber are contained in a report by Thiokol Chemical Corp. (RMD 5088-5098-S, Contract No. NAS 7-451). By making some guesses concerning the units used in that report, we calculate their permeation coefficient for CO_2 at 25°C to agree with our value within 3%.

In Table 3 the CO_2 permeation data for the nitroso rubber are compared with those of polyisoprene and of low density polyethylene; they are taken from the Polymer Handbook.

Table 3

COMPARISON OF CO_2 PERMEATION AND DIFFUSION DATA OF THREE POLYMERS

	$D_{25°} \times 10^7$ (cm_2/sec)	$P_{25°} \times 10^9$ $\left(\frac{cc\ cm}{cm^2\ sec\ cm\ Hg}\right)$	E_D (kcal/mole)	E_P (kcal/mole)
Nitroso rubber	6.8	15.2	6.4	5.1
Polyisoprene	10.5	13.9	8.9	6.2
Polyethylene	3.7	1.3	9.2	9.3

It is seen that the nitroso rubber is very permeable, comparable to an amorphous hydrocarbon rubber.

The interaction of NO_2-N_2O_4 with the rubber was explored also. Our source of the permeant was an N_2O_4 cylinder which was kept at about 30°C. Since the boiling point of N_2O_4 at 1 atm is 21°C, a sufficient overpressure is generated to drive the vapor through the permeation cell. (The emerging N_2O_4 is either condensed in a dry ice trap or absorbed in water.) The permeant passing into the He stream is present as pure NO_2 because of its low partial pressure (always well below 0.1%). The detector sensitivity for NO_2 was assumed to be the same as that for CO_2.

One permeation run was carried out at 48.2°C. From the steady state signal, which was reached after about 1-1/2 hr, a permeation coefficient of 1.9×10^{-7} $\frac{cc(stp)cm}{cm^2 \cdot sec \cdot cm\ Hg}$ was calculated. A nominal diffusion coefficient of 7×10^{-7} cm^2/sec was derived by our standard method. However, this number has at best only a semiquantitative significance, since two species, NO_2 and N_2O_4, are present. Thus the diffusion process is complex, and our simple procedure for determining D is questionable.

When the sample was degassed, extensive tailing was observed; after the signal had dropped to about half its value, several hours were required to reach the base line again. Thus sorption of NO_2-N_2O_4 by nitroso rubber does not appear to be reversible. The observed effects were shown to be due to the polymer itself, and not to slow sorption processes of NO_2 on the system walls: 1 to 50 µl of air and, in parallel experiments, NO_2-N_2O_4 were injected with a microsyringe into the carrier gas stream. For both gases, the appearance time of the signal was the same, the peaks were symmetrical, and the peak heights were approximately proportional to the amount injected.

C. Silicone Membrane (SR 6750-1)

The hydrogen permeation was investigated over a temperature range of 50 to 101°C. The data are shown in Table 4. The heats of permeation E_P and diffusion E_D were found to be E_P = 3.1 and E_D = 2.5 kcal/mole, and the permeation and diffusion coefficients at 50°C were

$$P_{50} = 5.2 \times 10^{-8} \frac{cc(stp)cm}{cm^2 \text{ sec cm Hg}}$$

and

$$D_{50} = 4.5 \times 10^{-5} \text{ cm}^2/\text{sec}$$

Table 4

HYDROGEN PERMEATION DATA
FOR SILICONE MATERIAL (SR 6750-1)

t (°C)	D × 10^5 (cm^2/sec)	P × 10^8 $\left(\frac{cc(stp)cm}{cm^2 \text{ sec cm Hg}}\right)$	S × 10^3 $\left(\frac{cc(stp)}{cm^3 \text{ cm Hg}}\right)$ (calculated)
101.1	7.50	9.94	1.32
91.7	7.12	8.90	1.25
80.1	6.38	7.74	1.21
70.3	5.68	6.82	1.20
63.5	5.37	6.24	1.16
50.1	4.54	5.18	1.14

D. Krytox Coating on Teflon

We explored whether a Krytox coating would reduce permeation rates through Teflon. A 4.4-mil Teflon membrane, of the same origin as those used in the principal studies, was mounted in our permeation unit, and the permeation rate of CO_2 was determined at five temperatures. The values agreed within 5% with the previously reported data. A 3-wt % solution of Krytox in Freon TF was then applied to the membrane in situ and the solvent evaporated. The average thickness of the residue was

about 0.5 mil. The coating was not uniform because the membrane was not perfectly flat; visual inspection indicated, however, that some material was deposited over the entire surface. The membrane was then carefully degassed and the permeation of CO_2 was remeasured at two temperatures. The permeation rates were, within the precision of the measurements, identical with those for the coated membrane.

E. Permeation and Diffusion of CO_2 and O_2 Through FEP Coated Glass Cloth

Permeation and diffusion measurements were carried out on samples of glass cloth inpregnated with FEP. The glass fibers had a diameter of 0.7 mil and the open areas between the fibers were about one-half of the total area. The thickness of the glass-supported FEP membrane was calculated from its weight to be 5.5 mil. The directly measured thickness, which varied by about 20% since the glass cloth was not uniformly embedded in the plastic, was about 8 mil. The value 5.5 mil was used for the calculations.

Diffusion and permeation of CO_2 and O_2 were measured at 65.0, 50.0, and 34.5°C. Reasonably straight Arrhenius plots were obtained. In Table 5, diffusion and permeation coefficients at 25°C, obtained by extrapolation of the Arrhenius plots, and the heat of diffusion and permeation of glass-supported FEP are compared with those of unsupported FEP. The agreement is surprisingly good if one considers the uncertainties in the present measurements. Thus the glass cloth may impart additional strength to the FEP membrane without changing its transport properties.

Table 5

COMPARISON OF TRANSPORT PROPERTIES OF
GLASS-CLOTH-SUPPORTED FEP(1) AND UNSUPPORTED FEP(2)

Gas	$D_{25} \times 10^7$ (cm^2/sec)		E_D (kcal)		$P_{25} \times 10^9$ $\frac{cc(STP)cm}{cm^2\ sec\ cm\ Hg}$		E_P (kcal)	
	1	2	1	2	1	2	1	2
CO_2	0.94	1.05	8.40	8.75	1.00	1.27	5.3	5.2
O_2	1.50	1.84	8.40	8.29	0.50	0.49	5.2	6.1

Appendix A*

DIFFUSION AND PERMEATION OF OXYGEN, NITROGEN, CARBON DIOXIDE, AND NITROGEN DIOXIDE THROUGH POLYTETRAFLUOROETHYLENE

by

R. A. Pasternak, M. V. Christensen, and J. Heller
Polymer Chemistry Program
Stanford Research Institute
Menlo Park, California 94025

ABSTRACT

The permeation of CO_2, O_2, N_2, and N_2O_4-NO_2 equilibrium mixtures through polytetrafluoroethylene (PTFE) has been investigated systematically. PTFE membranes between 1.5 and 5.7 mil thick were studied over a temperature range of 30 to 116°C. For all the gases, the permeation and diffusion coefficients were found to be independent of membrane thickness, within the precision of the measurements. Linear Arrhenius plots were obtained for CO_2, O_2, and N_2. For the N_2O_4-NO_2 system, the temperature dependence of both permeation and diffusion was complex; the permeation data could be explained quantitatively in terms of the N_2O_4-NO_2 equilibrium.

The parameters describing the diffusion and solution process indicate that the CO_2, O_2, N_2, and N_2O_4 molecules do not significantly interact with PTFE but move through preexisting channels and voids, whereas NO_2 interacts strongly, though reversibly, with the polymer.

---

* Published in Macromolecules 3, 366 (1970).

DIFFUSION AND PERMEATION OF OXYGEN, NITROGEN, CARBON DIOXIDE, AND NITROGEN DIOXIDE THROUGH POLYTETRAFLUOROETHYLENE

R. A. Pasternak, M. V. Christensen, and J. Heller
Polymer Chemistry Department
Stanford Research Institute
Menlo Park, California 94025

Introduction

The development of advanced liquid propulsion systems requires the use of expulsion bladders for storable propellants in the space environment. The bladder material must not only be chemically inert toward strong oxidants such as nitrogen dioxide but must also have a very low permeability toward these agents. Because of its chemical resistance and good mechanical properties, polytetrafluoroethylene (PTFE) has received serious consideration as a bladder material and several space vehicles have been launched using PTFE expulsion bladders.

However, permeation of oxidants through PTFE, while not detrimental in short missions, is of serious concern in long missions. Since only very limited data for the diffusion and permeation of noncondensible gases and none for nitrogen dioxide through PTFE are found in the literature,[1,2] a systematic study of these gases was undertaken in an attempt to understand the details of the interaction between permeants and PTFE.

Experimental

The dynamic method for measuring permeation and diffusion rates of gases and vapors in polymer membranes has been described in detail elsewhere[3] and is here only summarized. The two compartments of the permeation cell, which are separated by the test membrane, are open to the atmosphere. The permeant, gas or vapor, is admitted to one compartment, replacing a carrier gas, usually helium. A second carrier gas stream flows at constant rate through the other compartment and sweeps the

permeant, which diffuses through the membrane, to the thermal conductivity detector. The detector signal, which is originally zeroed with the carrier gas in both compartments, is at any instant proportional to the permeation rate. When the permeant is again replaced by the carrier gas, the membrane is degassed, and the signal returns to the base line. Thus, repeat measurements can be made with the same membrane over a wide temperature range and for diverse permeants.

The instrument used in this study is a prototype of the Polymer Permeation Analyzer (PPA).* The cell and the plumbing were stainless steel; the effective membrane area was 3.9 cm^2. The detector was a Loenco* thermal conductivity cell which was run at 140 mA and thermostated at 80°C. Its sensitivity for CO_2, 144 ppm/mV, did not change significantly with time, even after exposure to NO_2. The combination of the detector with a Sargent recorder (full scale deflection of 250 mm at an input of 0.4 mV) resulted in a detection limit of 0.2 ppm of CO_2 in helium. Helium was used as carrier gas for the study of all permeants, except of hydrogen, for which nitrogen was used. (With N_2 as carrier gas the detector current was 50 mA.) The flow rates of the carrier gas were set between 0.5 and 1.5 ml/min, the higher values being employed at high diffusion rates. At steady-state permeation, strict inverse proportionality between signal and flow rate was found as expected for a detector with linear response.

The detector sensitivity, which is a function of the gas or vapor sensed, was determined for CO_2 and H_2O. Helium with 0.21 vol % CO_2 and nitrogen with 0.20 vol % H_2, were used as test gases. Moreover, the permeation rates of CO_2, O_2, and N_2 through a PTFE membrane were measured in a Barrer-type permeation cell (Linde Model CS 135), and compared with the equivalent signals obtained in the PPA. The permeation coefficients for CO_2 derived by the two independent approaches differed by 7%; the data reported here are based on the calibration of the PPA. The mole response factors of the detector for O_2 and N_2 (relative to CO_2) were found to be 1.20 and 1.22; the factor for NO_2 was assumed to be unity because its

* Manufactured by Dohrmann Instrument Co. (Infotronics), Mt. View.

molecular weight differs by only two units from that of CO_2. No N_2O_4 reached the detector since in the helium stream the highest partial pressure of the nitrogen oxides, expressed as NO_2, was less than 0.1%. Finally, the equilibrium solubility of N_2O_4-NO_2 in PTFE at a total pressure of one atmosphere was measured over a limited temperature range with a quartz spring balance.

High purity CO_2, O_2, and N_2 were used without further purification or drying; the N_2O_4-NO_2 mixture was bled into the cell from a tank held at 30°C. The PTFE used in this study had a density of 2.18 g/cc at 18°C as determined by immersion in water. Membranes were cut with a microtome from a solid polymer block of Dupont Teflon, commercial stock, and their thicknesses were determined by a micrometer with a reading precision of 0.05 mil. Only membranes with thickness variation of less than 5% were used.

Evaluation of Permeation and Diffusion Coefficients

In Fig. 1a, a typical permeation curve for CO_2 is shown. The plateau represents steady-state permeation. The permeation coefficient P is calculated by the formula

$$P = \frac{f \cdot \sigma \cdot k \cdot a \cdot S_\infty \cdot \ell}{A \cdot p} \quad \left(\frac{cc \cdot cm}{cm^2 \cdot sec \cdot cm\ Hg}\right)$$

where f is the flow rate, σ the detector sensitivity, k the Molecular Response Factor, a the detector attenuation, S_∞ the steady-state signal, ℓ the membrane thickness, A the membrane area, and p the upstream permeant pressure. The permeant pressure is taken as 76 cm Hg although it varied slightly.

The steady-state data for N_2O_4-NO_2 are reported as the measured flux of NO_2 at a total pressure of one atmosphere, normalized to unit area and thickness. Formalistically, the flux is identical to a nominal permeation coefficient at atmospheric pressure.

The diffusion coefficient was derived from the ascending and descending branches of Fig. 1a which represent the transient permeation rates.

The solution of the differential equation describing the transient state has been discussed in detail elsewhere.[3] It is to a good approximation

$$\frac{S}{S_\infty} = \frac{4}{\sqrt{\pi}} \cdot X \cdot \exp(-X^2)$$

where $X^2 = \ell^2/4Dt$, S is the signal at time t, and D is the concentration-independent diffusion coefficient. This equation describes both sorption and degassing, which are identical except for reversal in the direction of the signal. A plot of S/S_∞ vs $1/X^2$ is the theoretical, normalized, permeation rate curve. If, for the same values of S/S_∞, the normalized times $1/X^2$ are plotted vs the experimental times t, the straight line through the origin should have a slope equal to $4D/\ell^2$. Figure 1b represents this evaluation of the ascending and descending branches of Fig. 1a. The points lie on a straight line, and close agreement is found between the two branches. However, a positive displacement on the time axis is found, because a finite time is required for the permeant to reach the upper compartment, and for the permeated gas to reach the detector.

A simplified method has been adopted for the evaluation of the large amount of data. The slope, which is given by the ratio $\frac{\Delta 1/X^2}{\Delta t}$, was evaluated from two sets of two experimental points each, namely for S/S_∞ = 0.1, 0.4 and S/S_∞ = 0.4, 0.7. For the noncondensible gases, the two values agreed within 5% and were averaged.

For the NO_2-N_2O_4 system the determination of diffusion coefficients by the described formalism becomes questionable. The simultaneous diffusion of two interacting components must result in a complex rate law; unfortunately, the differential equation cannot be solved explicitly in this case. The experimental curves have shapes similar to those for the noncondensible gases (Fig. 2a); however, plots of $1/X^2$ vs t (Fig. 2b), though approximately linear, show a slight curvature and they intercept the time axes at negative values. Both effects diminish with increasing temperature, as would be expected from a consideration of the N_2O_4-NO_2 equilibrium. The nominal diffusion coefficients reported here were somewhat arbitrarily derived from the slopes for the interval S/S_∞ = 0.1, 0.4,

Results and Discussion

1. Carbon Dioxide, Oxygen, and Nitrogen

In Fig. 3 the logarithm of the permeation coefficients for CO_2, O_2, and N_2 derived from the data are plotted versus $1/T$; Fig. 4 is an equivalent plot of the diffusion coefficients. For CO_2, membranes of thickness 1.5, 3.2, 3.5, 4.3, and 5.7 mil were used, but no diffusion coefficients are given for the thinnest membrane, since the transient permeation rate was too fast to yield reliable values. The 1.5-mil membrane was omitted in the O_2 and N_2 studies.

The complete data cover a temperature range of 30 to 116°C; however, the individual membranes were studied over smaller intervals, the range depending on the membrane thickness. Also, for any given membrane, permeation coefficients are usually given to higher temperatures than diffusion coefficients because the determination of the latter becomes unreliable for fast transient rates.

Since the agreement between the data for different membranes was very good, they were all combined in a least square treatment. The straight lines in the figures represent the results. The mean square root deviation of the individual data points from the best line is between 3 and 5% for all plots. Deviations for an individual membrane do not appear to be systematic or significant, and are well within the range of uncertainties originating from thickness measurement and slight variation in flow rate of the carrier gas.

In Table 1 the diffusion and permeation coefficients at 25°C, D_{25} and P_{25}, the preexponential factors D_0 and P_0, and the heats E_D and E_P, are summarized. In addition, the solubility coefficients calculated from $s = P/D$ are listed. The permeation coefficient and the heat of permeation of H_2, which was measured for one membrane only and at four temperatures between 24 and 48°C, are included. Permeation coefficients for the four gases in FEP given in the literature[2] are shown also.

The diffusion and permeation coefficients of CO_2, O_2, and N_2, plotted in Figs. 3 and 4, confirm convincingly that the generally assumed simple

Table 1

DIFFUSION, PERMEATION, AND SOLUBILITY DATA FOR NONCONDENSIBLE GASES IN PTFE

Gas	$D_{25} \times 10^7$	$D_0 \times 10^2$	E_D	$P_{25} \times 10^9$	$P_0 \times 10^6$	E_P	$s_{25} \times 10^2$	$s_0 \times 10^4$	ΔH_s	$P_{25} \times 10^9$*
CO_2	0.95	1.03	6.84	1.17	0.33	3.34	1.230	0.323	-3.50	1.00
O_2	1.52	0.64	6.28	0.42	0.93	4.55	0.276	1.48	-1.73	0.45
N_2	0.88	1.52	7.12	0.14	2.69	5.82	0.159	1.76	-1.30	0.19
H_2				0.98		5.10				1.30

D_{25} and D_0 in cm^2/sec; P_{25} and P_0 in $\frac{cc(STP)cm}{cm^2\ sec\ cm\ Hg}$; s_{25} and s_0 in $\frac{cc(STP)}{cm^3\ cm\ Hg}$; E and ΔH in kcal/mole.

The diffusion coefficient at absolute temperature T is given by $D = D_0 \exp \frac{-E_D}{RT}$. Analogous expressions apply to the permeation coefficient P and the solubility s. The subscript 25 signifies the value at 25°C.

* FEP Ref. 2.

diffusion law holds; the independence of the coefficients on membrane thickness, in particular, proves that the sorption process on the membrane surface is fast and is not the rate determining step. The data also show that the activation energies of diffusion and permeation are independent of temperature, over the rather wide temperature range of this study.

The activation energies of diffusion E_D of the three gases (Table 1) are quite similar. However, in view of the high precision of the data, the differences, though small, are significant. This is also indicated by the trend in the preexponential factors; their logarithms, i.e., the entropies of activation, are approximately a linear function of the activation energies of diffusion, as has been found in other systems.[1] The trend in E_D appears to be associated with the molecular sizes of the gases. Oxygen has a significantly smaller Van der Waal's diameter (2.92Å) than N_2 (3.15Å) and CO_2 (3.23Å).[4] Moreover, since the cross section perpendicular to the molecular axis is smaller for CO_2 than for N_2, the lower E_D value for CO_2 may indicate that the molecules permeate by preference in the direction of their molecular axis.

The heats of solution of the three gases in PTFE and their heats of condensation (last column) are compared in Table 2. The close numerical agreement is probably fortuitous; nevertheless it indicates that solution in PTFE is similar to a condensation process with minimal interaction between the polymer and the solute.

A comparison of diffusion and solubility data of PTFE with those of the structurally similar linear polyethylene is of some interest (Table 2). The polyethylene data are for a Phillips type 22% amorphous polymer and are taken from two papers by Michaels and Bixler[5]; they are converted to the units used here. The solubilities refer to the amorphous phase and are calculated assuming the solubility in the crystalline phase to be negligible. The PTFE used was 40% amorphous as determined from its density.

The activation energy of diffusion of the three gases in PTFE is about two kcal/mole lower than in polyethylene. This is surprising, since PTFE has very stiff backbone chains of high viscosity. Apparently, as proposed

Table 2

DIFFUSION AND SOLUBILITY DATA OF PTFE (T)
AND OF LINEAR POLYETHYLENE (PE)*

Gas	E_D		$S_{25} \times 10^2$		ΔH_s		ΔH_{cond}
	T	PE	T	PE	T	PE	
CO_2	6.84	8.5	3.1	0.60	-3.50	-1.3	-4.0†
O_2	6.28	8.8	0.69	0.10	-1.73	-0.4	-1.6
N_2	7.12	9.0	0.39	0.054	-1.30	0.5	-1.3

Note: ΔH in kcal/mole; s_{25} in $\frac{\text{cc STP}}{\text{cm}^3 \text{ cm Hg}}$

* Ref. 5.
† At triple point, -56°C.

originally by Brandt and Anysas,[1] diffusion of small molecules in this polymer proceeds through preformed channels and cavities and requires little movement of the polymer chains.

The higher gas solubilities at 25°C, more than six times those in polyethylene, and the higher heats of solution may again indicate poor packing of the PTFE chains in the amorphous regions.

2. Nitrogen Dioxide

Figure 5 summarizes the data for the N_2O_4-NO_2 system obtained with the same five membranes as for CO_2. Repeat runs were reproducible even after long time exposure of the membranes to the strong oxidant. Moreover, data for CO_2 obtained before and after exposure to NO_2 were identical within the precision of the measurements, evidence that PTFE is not attacked by NO_2. The nominal diffusion coefficients (see preceding section) lie on a straight line (curve 1) except at the lower temperatures. The steady-state permeation data closely fit the theoretical curve 2 (see below), except for some points for the 4.3-mil membrane at lower temperatures.

Finally, in Table 3 the solubilities of the N_2O_4-NO_2 equilibrium mixtures at a total pressure of one atmosphere are given for two PTFE samples; the agreement is quite satisfactory.

Table 3

SOLUBILITY IN PTFE OF N_2O_4-NO_2
EQUILIBRIUM MIXTURE AT 1 ATM PRESSURE

T (°C)	s(g/cc Atm)		s(cc NO_2(STP)/cc Atm) (average)
	Sample 1	Sample 2	
30.1	0.039	0.038	19.0
35.4	0.027	--	13.0
40.6	0.019	0.020	9.5

The close agreement of the apparent diffusion coefficients and the normalized permeation rates for different membrane thicknesses, shown in Fig. 5, indicate again that the adsorption process is fast, and that the transport within the membrane is the rate determining step. This transport mechanism however is complex not only because two species diffuse, but also because the relative concentrations of N_2O_4 and NO_2 in the gas phase and in the polymer are functions of temperature and total pressure (or concentration).

The equilibrium in the gas phase is given by[6]

$$\frac{(p_{NO_2})^2}{p_{N_2O_4}} = K_p = 7.1 \times 10^9 \exp \frac{-14,600}{RT} \text{ Atm} \qquad (1)$$

At a total pressure of one atmosphere on the upstream side of the membrane (our standard experimental condition) the partial pressure of NO_2 is 0.36 atm at 30°C, and 0.99 atm at 116°C. (On the downstream side, virtually pure NO_2 is released since the total pressure of permeant in the helium stream was in all experiments below 10^{-3} atm.)

Since at the highest temperatures of this study the gas phase consists of virtually pure NO_2, it is reasonable to assume that the measured nominal diffusion and permeation coefficients are the true coefficients for NO_2. Actually, the diffusion coefficient curve is at the higher temperatures linear over a much wider interval than anticipated. The diffusion parameters derived from it are ascribed to NO_2 and listed in Table 4.

Table 4

DIFFUSION, PERMEATION, AND SOLUBILITY DATA
FOR NO_2 AND N_2O_4 IN PTFE
(For Units and Definitions, see Table 2)

Gas	$D_{25} \times 10^7$	D_o	E_D	$P_{25} \times 10^9$	$P_o \times 10^6$	E_P	$s_{25} \times 10^2$	$s_o \times 10^9$	ΔH_s
NO_2	0.037	70	14.0	1.57	0.116	2.55	43	1.66	-11.4
N_2O_4	0.25	--	--	3.75	0.0013	-0.5	15	--	--

In our analysis of the observed nonlinear temperature dependence of permeation, we make the following postulates: (1) the solubility of either component obeys Henry's Law

$$C_i^o = s_i \cdot p_i \qquad (2)$$

where C_i^o is the saturation concentration in the polymer, s_i is the solubility coefficient, and p_i is the pressure in the gas phase; (2) both the diffusion and solubility coefficients are independent of concentration. This postulate probably holds only approximately since the total equilibrium amount of $NO_2 + N_2O_4$ dissolved at the lowest temperature of the experimental series is about 2% by weight; (3) the equilibrium $N_2O_4 \rightleftarrows 2NO_2$ is maintained at all times in the gas phase and everywhere within the membrane, even during transient permeation.

It follows from the three postulates that the concentrations C_i anywhere in the polymer satisfy, at all times, the equilibrium condition

$$\frac{\left(C_{NO_2}\right)^2}{C_{N_2O_4}} = K_c = K_p \frac{s_{N_2O_4}}{\left(s_{NO_2}\right)^2} \tag{3}$$

Diffusion through the membrane is described by the two differential equations

$$\frac{dC_{NO_2}}{dt} = -D_{NO_2} \frac{d^2C_{NO_2}}{dx^2} + 2R \tag{4a}$$

$$\frac{dC_{N_2O_4}}{dt} = -D_{N_2O_4} \frac{d^2C_{N_2O_4}}{dx^2} - R \tag{4b}$$

R is the net rate of conversion of N_2O_4 to NO_2; the factor 2 in Eq. (4a) accounts for the production of two NO_2 molecules for every dissociating N_2O_4 molecule.

Equations (4a) and (4b) are not independent, but are related by Eq. (3). By combining these three equations, a differential equation in C_{NO_2}, time t, and position x can be obtained. Unfortunately, this equation cannot be solved except numerically, and therefore the diffusion coefficients cannot be derived explicitly from the experimental curves. However, a solution can be obtained for the steady state, when the concentrations of both NO_2 and N_2O_4 anywhere in the membrane are independent of time. The flux F of permeant through the membrane of thickness ℓ

$$F = -D_{NO_2} \frac{dC_{NO_2}}{dx} - 2D_{N_2O_4} \frac{dC_{N_2O_4}}{dx} \tag{5}$$

is then constant, i.e., also independent of x. The factor 2 has been introduced to express the flux in terms of the NO_2 species, which appears exclusively on the downstream side of the membrane.

At steady state the boundary conditions are

$$\text{at } x = 0 \qquad C_{NO_2} = C^o_{NO_2}$$

$$C_{N_2O_4} = C^o_{N_2O_4}$$

$$\text{at } x = \ell \qquad C_{NO_2} = C_{N_2O_4} = 0$$

Integration of Eq. (5) between these limits yields

$$F \cdot \ell = D_{NO_2} C^o_{NO_2} + 2D_{N_2O_4} C^o_{N_2O_4} \tag{6}$$

On introducing Henry's Law, Eq. (1), we obtain

$$F \cdot \ell = D_{NO_2} s_{NO_2} p_{NO_2} + 2D_{N_2O_4} s_{N_2O_4} p_{N_2O_4} \tag{7}$$

We define: the flux at unit thickness $F_0 = F \cdot \ell$, and

the permeation coefficients $P_{NO_2} = D_{NO_2} s_{NO_2}$;

$$P_{N_2O_4} = D_{N_2O_4} s_{N_2O_4}$$

Since in our experiments the pressure condition holds

$$p_{NO_2} + p_{N_2O_4} = 1 \text{ atm},$$

the flux equation assumes the simple form

$$F_0 = p_{NO_2} P_{NO_2} + 2(1-p_{NO_2}) P_{N_2O_4} \tag{8}$$

Formalistically this equation is identical with the expression that describes the permeation of two independent components; however, in the NO_2-N_2O_4 case, the concentrations of the two species in the membrane are not linear functions of x but are related by the mass law.

It can be easily seen that the permeation data plotted in Fig. 5 are in the form of this normalized flux F_0; they can be analyzed in terms of Eq. (8). We postulate that both P_{NO_2} and $P_{N_2O_4}$ show an exponential dependence on the reciprocal temperature. Since at the highest temperatures of the experiments the gas phase is virtually pure NO_2, the permeation coefficients P_{NO_2} are given by the asymptote to the high temperature data, curve 3 in Fig. 5, and can be extrapolated to lower temperatures. Moreover, the partial pressures of p_{NO_2} are given by equilibrium Eq. (1). Consequently, only the permeation coefficient $P_{N_2O_4}$ of Eq. (8) is unknown and can be calculated at different temperatures from the smoothed, experimental F_0 values. After minor adjustments in the slope of the P_{NO_2} curve, a linear $P_{N_2O_4}$ curve was obtained [(4) in Fig. 5)]. Then, as a check, the total flux F_0 was recalculated from the two permeation curves (3) and (4). The agreement of the calculated curve (2) with the experimental data is excellent, except for some points derived from the 4.3-mil membrane.

The parameters derived from the two permeation curves (3) and (4) are listed in Table 4. The coefficients, which in Fig. 5 are given in atmospheric pressure units, are converted to cm Hg units to facilitate comparison with the CO_2, O_2, and N_2 data. Approximate solubility and diffusion coefficients of N_2O_4 at 25°C are given also. The solubility coefficient was derived from the directly measured solubilities (Table 2) by extrapolation to 25°C. A correction was made for the solubility of the NO_2 present in the gas phase at 25°C.

A comparison of the solubility and diffusion coefficients of N_2O_4 and of CO_2, O_2, N_2 indicates a common pattern. The solubility coefficients of the gases correlate quite well with their boiling points, as has been found for other gas-polymer systems.[7] Similarly, the reduction in the N_2O_4 diffusion coefficient by a factor of about 4 compared to CO_2 appears to be reasonable in view of the much larger size of the N_2O_4 molecule. Thus, N_2O_4, like the other gases, apparently does not interact with PTFE.

In contrast, the NO_2 data do not fit the pattern at all. Although the NO_2 molecule has approximately the same size as CO_2, its activation energy of diffusion is about twice and its heat of solution about three times that of CO_2. Also, its diffusion and solubility coefficients at 25°C are smaller and larger, respectively by orders of magnitude. These observations suggest that the highly polar NO_2 molecule interacts strongly with PTFE.

A systematic analysis of the data in terms of molecular dimensions and interchain forces is not only of considerable interest, but is essential for a more detailed and quantitative understanding of diffusion mechanisms. This analysis must however be postponed until data for a larger number of permeants and PTFE samples of different degree of crystallinity are available.

Acknowledgment

The authors are indebted to Mr. David D. Lawson for suggesting this research and for preparing suitable membranes. This work was performed for the Jet Propulsion Laboratory, California Institute of Technology, sponsored by the National Aeronautics and Space Administration under Contract NAS 7-698.

REFERENCES

1. W. W. Brandt and G. A. Anysas, J. Appl. Polymer Sci., 7, 1919 (1963).
2. Modern Plastics Encyclopedia, 1968/69, p 525.
3. R. A. Pasternak, J. F. Schimscheimer, and J. Heller, J. Polymer Sci., Part A2, in press.
4. Handbook of Chemistry and Physics, 36th Ed., p 3094 (1955).
5. A. S. Michaels and H. T. Bixler, J. Polymer Sci., 50, 393, 413 (1961).
6. Physical Chemistry by F. H. Getman and F. Daniels, Wiley & Sons, Inc., New York, N. Y., 1946, p 297.
7. G. T. van Amerongen, Rubb. Chem. Technol. 37, 1065, (1964).

ILLUSTRATIONS

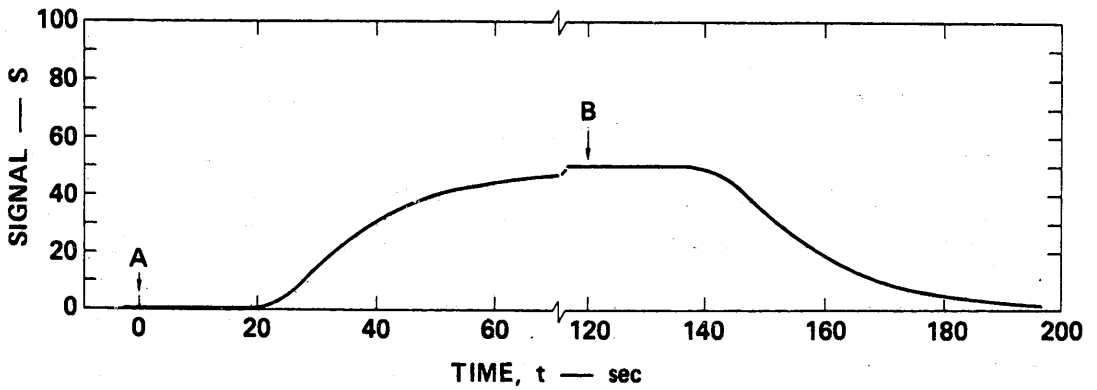

TA-7758-1s

FIGURE 1a

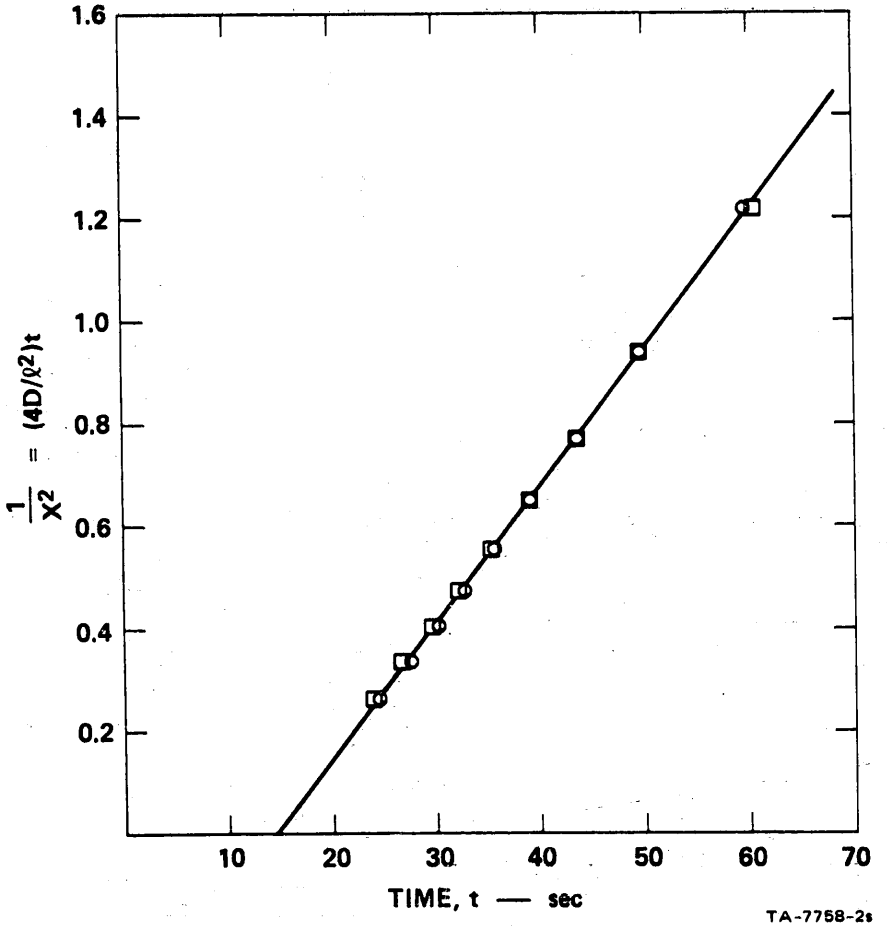
1.6
1.4
1.2
1.0
0.8
0.6
0.4
0.2
$\frac{1}{X^2} = (4D/\ell^2)t$
10
20
30
40
50
60
70
TIME, t — sec
TA-7758-2s

FIGURE 1b

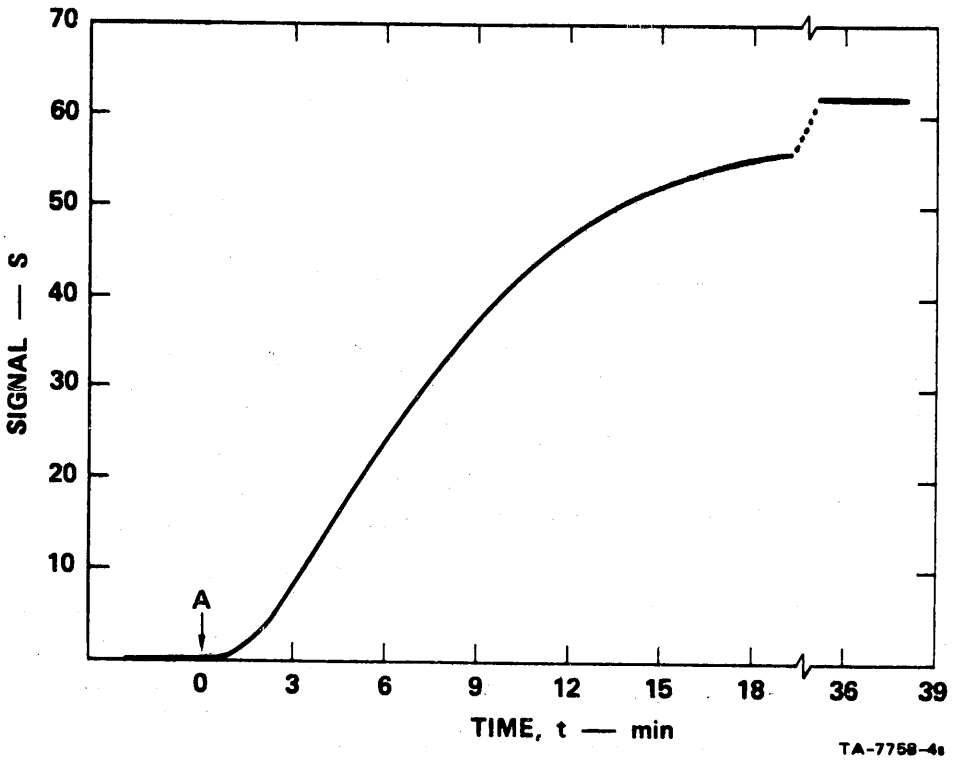
70
60
50
40
30
20
10
SIGNAL — S
A
0
3
6
9
12
15
18
36
39
TIME, t — min
TA-7758-4s

FIGURE 2a

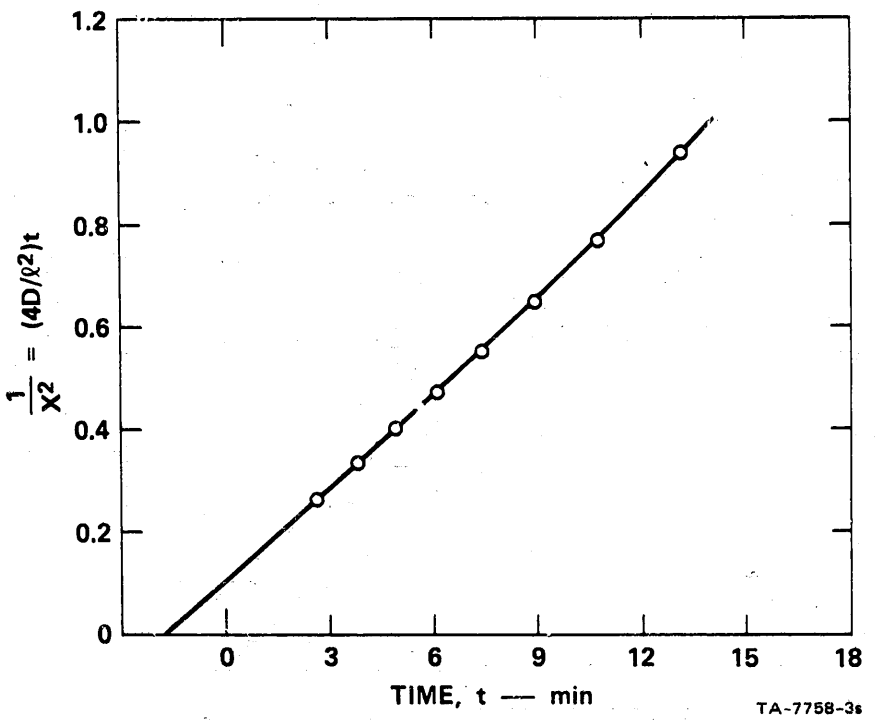
1.2
1.0
0.8
0.6
0.4
0.2
0
$\frac{1}{X^2} = (4D/\ell^2)t$
0
3
6
9
12
15
18
TIME, t — min
TA-7758-3s

FIGURE 2b

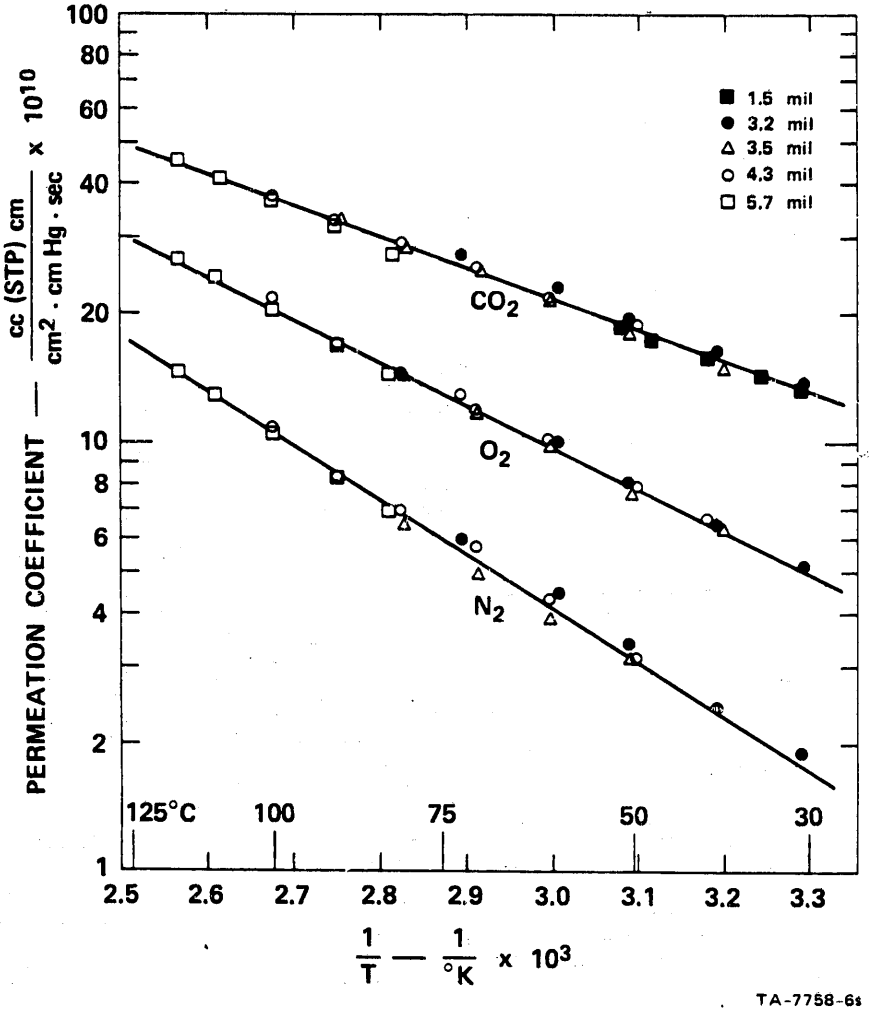
PERMEATION COEFFICIENT — cc (STP) cm / cm² · cm Hg · sec x 10¹⁰
100
80
60
40
20
10
8
6
4
2
1
1.5 mil
3.2 mil
3.5 mil
4.3 mil
5.7 mil
CO2
O2
N2
125°C
100
75
50
30
2.5
2.6
2.7
2.8
2.9
3.0
3.1
3.2
3.3
1/T — 1/°K x 10³
TA-7758-6s

FIGURE 3

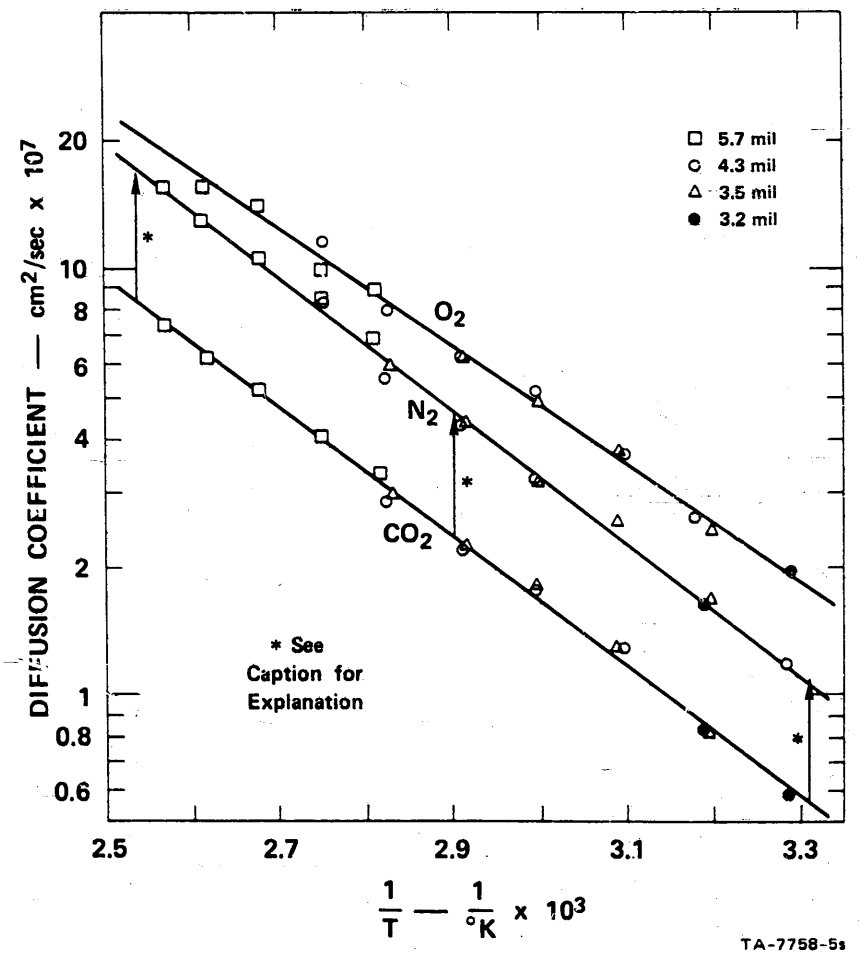
DIFFUSION COEFFICIENT — cm²/sec x 10⁷
20
10
8
6
4
2
1
0.8
0.6
2.5
2.7
2.9
3.1
3.3
1/T — 1/°K x 10³
5.7 mil
4.3 mil
3.5 mil
3.2 mil
O2
N2
CO2
* See Caption for Explanation
TA-7758-5s

FIGURE 4

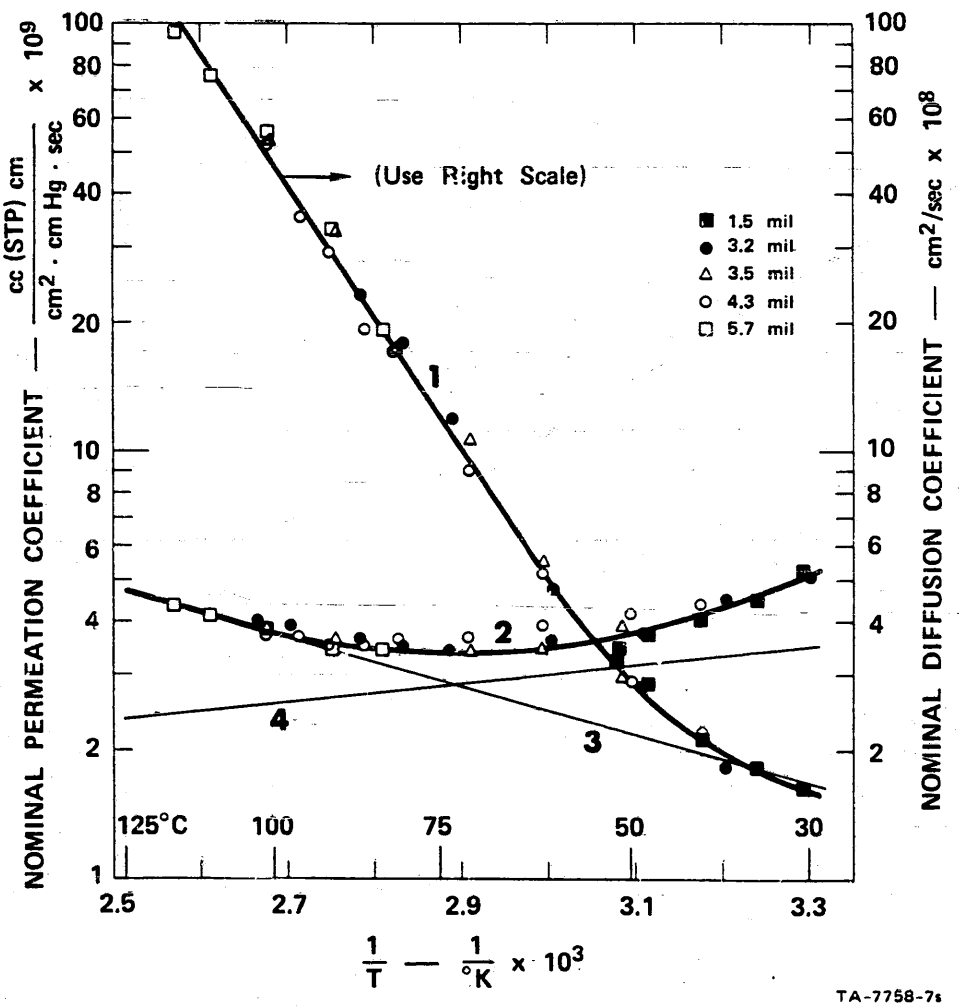
NOMINAL PERMEATION COEFFICIENT — cc (STP) cm / cm² · cm Hg · sec x 10⁹
NOMINAL DIFFUSION COEFFICIENT — cm²/sec x 10⁸
(Use Right Scale)
1.5 mil
3.2 mil
3.5 mil
4.3 mil
5.7 mil
1
2
3
4
125°C
100
75
50
30
2.5
2.7
2.9
3.1
3.3
1/T — 1/°K x 10³
TA-7758-7s

FIGURE 5

Appendix B*

DIFFUSION AND SOLUBILITY OF SIMPLE GASES THROUGH A COPOLYMER OF HEXAFLUOROPROPYLENE AND TETRAFLUOROETHYLENE

by

R. A. Pasternak, G. L. Burns, and J. Heller
Polymer Chemistry Program
Stanford Research Institute
Menlo Park, California 94025

ABSTRACT

The transport of seven gases, N_2, O_2, CO_2, CH_4, C_2H_6, C_3H_8, and C_2H_4, through FEP, a copolymer of hexafluoropropylene and tetrafluoroethylene, has been studied systematically over a temperature range of about 25 to 85°C. For all the gases studied, linear Arrhenius plots of both permeation and diffusion coefficients were obtained. Empirical linear correlations both between the logarithm of the solubility at 25° and the heat of solution, and the Lennard-Jones force constant of the gases were found. Furthermore, the standard entropies of solution and of diffusion were linearly dependent on the associated enthalpies. A comparison of the FEP data with those for polyethylene taken from the literature points up the limitations of existing theories of transport through polymers. Finally, the comparison with data on polytetrafluoroethylene (PTFE) indicates that the properties of the latter may be due at least in part, to micropores or grain boundaries.

---

* To be published in Macromolecules.

DIFFUSION AND SOLUBILITY OF SIMPLE GASES THROUGH A COPOLYMER OF HEXAFLUOROPROPYLENE AND TETRAFLUOROETHYLENE

By R. A. Pasternak, G. L. Burns, and J. Heller
Stanford Research Institute
Menlo Park, California 94025

In a recent study of gas transport in polytetrafluoroethylene (PTFE) it was found that the activation energies of diffusion of N_2, O_2, and CO_2 were approximately 2 kcal/mole lower than they were in polyethylene (PE).[1] Since complete fluorination of polyolefins leads to considerable stiffening of the carbon backbone, this is an unexpected result which suggests that diffusion progresses partly through micropores in the PTFE. Such an explanation appears reasonable since PTFE of sufficiently high molecular weight to be usable does not flow in the melt above its crystalline melting point of 327°C; fabrication requires compacting PTFE powder under high pressure near room temperature and then sintering at temperatures around 380°C. The final product usually obtained by machining very likely contains micropores.

The present study of diffusion through a copolymer of hexafluoropropylene and tetrafluoroethylene (FEP) was undertaken partly to verify this postulated diffusion mechanism. FEP has a crystalline melting point near 290°C, and whereas it retains most of the properties of PTFE, it has a melt viscosity in a range which allows fabrication by conventional techniques. Thus, FEP films can be expected to be free of micropores.

Experimental Section

Measuring Method

The dynamic method for measuring permeation and diffusion rates of gases and vapors in polymer membranes and the evaluation of the permeation and diffusion coefficients from the raw data have been described

in detail elsewhere.[2,3] The instrument used here was an engineering model of the Polymer Permeation Analyzer.* This instrument is equipped with three permeation cells, which can accept membranes of different thickness, and thus it permits a wide choice of measuring conditions. A low volume valve permits selection of any of the three cells for study.

The instrument is well suited to rapid study of a series of gases over a wide temperature range. In actual operation, a gas at atmospheric pressure is admitted from a manifold to the upstream side of the thermostated cells; after completion of the measurements, the manifold is evacuated with a mechanical pump, and another gas is admitted and the procedure repeated.

As a test of reproducibility, the permeation rates of CO_2 at 35° through one piece of FEP mounted across all three cells were measured. They were found to agree within 2%, which is equal to the reproducibility of repeat measurements for one cell.

The concentration of permeant gas in the helium carrier gas sweeping past the membrane was measured with a katharometer. The absolute detector sensitivity for CO_2 was determined by means of a CO_2-He mixture of known concentration. The sensitivities for the other gases studied relative to CO_2 were determined directly by a method which will be described elsewhere.[4]

The measured sensitivities, which compare quite well with those given in the literature,[5] are:

CO_2, 1; O_2, 1.21; N_2, 1.14; CH_4, 1.32; C_2H_6, 0.97; C_2H_4, 0.98; C_3H_8, 0.80.

Gases

High purity bottled gases were used without drying. Ethane and ethylene were better than 99.0%, the other gases were 99.5 to 99.9% pure. It should be recognized that contamination of a slowly permeating gas with a

* Manufactured by Infotronics Instrument Corp., Mountain View, California.

rapidly permeating gas can greatly influence the data. For example, the permeation coefficient of C_3H_8 at 25° is about 1% of that of CO_2. Thus, a 1% contamination with CO_2 would nominally double the steady-state signal of C_3H_8. However, since a parallelism exists between permeation and diffusion coefficients, CO_2 appears on the downstream side long before C_3H_8, and two well-defined steps would be observed in the dynamic method used here. Indeed, a very low step preceding the main step was occassionally observed and was ascribed to contamination from the manifold.

Membranes

FEP membranes of different thickness obtained directly from DuPont and from local suppliers were compared at 35°C. Variations were found in the permeation coefficient for CO_2 of more than 10%, larger than the uncertainty in thickness measurements (0.05 mil). Three membranes were finally selected which had average thicknesses of 1.10, 1.87, and 5.26 mils. The permeation coefficients for the first two membranes were identical within the precision of the measurements, but that for the thick membrane was lower by about 10%. This discrepancy was found at all temperatures and for all gases, whenever a comparison could be made; the diffusion coefficients, however, did not appear to vary for the three membranes. The permeation data reported here are all derived from the 1.10-mil membrane; the diffusion data are combined from all membranes since, depending on the gas and the temperature, steady-state permeation might be reached too fast for the thin membranes, and too slow for the thick membranes to determine reliably the diffusion coefficients. In the present instrument, the time to reach half the steady-state signal must be at least 30 sec to allow evaluation of the curves in terms of diffusion coefficients.

The membranes were annealed for 24 hr at 95°C. No significant change in thickness was observed; however, both the permeation and diffusion coefficients at 35° had increased by about 10%. Occasional temperature cycling, between higher temperatures and 35° in the course of the study did not show further changes in the transport parameters.

Crystallinity

Since no data on the crystallinity of FEP were given by the manufacturer or in the literature, x-ray diffractometer spectra were taken for both FEP and PTFE. A few distinct lines were found superposed on diffuse bands which were identical for the two polymers; they are given in Table 1. Other lines are indicated but are barely distinguishable from the background.

Table 1

DIFFRACTION DATA FOR PTFE AND FEP,
INDEXED ACCORDING TO A HEXAGONAL LATTICE

hkl	PTFE			FEP		
	Peak Heights (arb units)	d (Å)	a = b (Å)	Peak Heights (arb units)	d (Å)	a = b (Å)
100	356	4.90	5.65	208	5.01	5.77
110	16	2.83	5.66	5	2.885	5.77
200	20	2.43	5.58	6	2.49	5.74
	20	2.18	--	--	--	--

Note: hkl are the indices, d the spacings, and a = b the hexagonal axes.

The first three lines listed fit well a hexagonal lattice, with axes of 5.63 and 5.76 Å for PTFE and FEP, respectively. The former value is close to 5.66 Å, reported previously.[6,7]

The close agreement in unit cell dimensions and the similar relative intensities of the lines suggest closely similar packing of the chains in the two polymers; apparently the bulky CF_3 groups of FEP can be accommodated in the crystal structure without increasing significantly the unit cell dimensions.

The lines of FEP were found to be significantly wider than those of PTFE. The crystallite sizes (in the a-b plane) estimated from the line width were about 200 Å for FEP and at least twice as large for PTFE.

To summarize, the FEP contains a significant fraction of a highly dispersed crystalline phase, though probably less than PTFE. However, the present data are not sufficient to make a quantitative estimate of this fraction.

Results

In Figs. 1 and 2 the logarithms of the permeation coefficients and of the diffusion coefficients, respectively, are plotted versus the reciprocal absolute temperatures. A temperature range of about 60^0 is covered by the data; except the steady-state permeation rates for C_3H_8 at the lowest two temperatures were too small to permit precise measurements. The straight lines drawn were obtained by least squares treatment of the data. The standard deviation of the data points from this line is about 2%, and the uncertainty in the slopes is of about the same magnitude; no systematic deviations are observed. However, both permeation and diffusion coefficients measured at 95^0C (not shown in the figures) lie significantly above the straight lines; these deviations were shown to be reversible by temperature cycling. We suspect a phase transition, which is also indicated by a discontinuity in the tensile modulus at about 80^0C.[8]

In Table 2 the permeation and diffusion coefficients P and D at 25^0 and the associated preexponential factors and energies are listed; they are derived from the straight line plots according to the equations

$$\begin{aligned} P &= P_o \exp(-\Delta E_P/RT) \\ D &= D_o \exp(-\Delta E_D/RT) \end{aligned} \qquad (1)$$

The solubilities and parameters associated with them, which are also shown, are calculated from the relationship

$$k = \frac{P}{D} = k_o \exp(-\Delta H_S/RT) \qquad (2)$$

The uncertainties in ΔE_P and ΔE_D are estimated to be about 0.2 kcal, and in ΔH_S about 0.3 kcal. Uncertainties in the preexponential factors are quite large because their determination involves a linear extrapolation

Table 2

DIFFUSION, PERMEATION, AND SOLUBILITY DATA FOR SEVEN GASES IN FEP

Gas	$D_{25} \times 10^{8}$	D_o	E_D	$P_{25} \times 10^{11}$	$P_o \times 10^{5}$	E_P	k_{25}	$k_o \times 10^{3}$	ΔH_S
N_2	9.48	0.522	9.20	15.9	3.65	7.31	0.127	5.30	-1.89
O_2	18.4	0.218	8.29	49.0	1.45	6.09	0.205	5.04	-2.20
CO_2	10.5	0.272	8.75	127.0	0.59	5.00	0.92	1.64	-3.75
CH_4	2.98	2.92	10.89	8.65	11.00	8.31	0.220	2.86	-2.58
C_2H_6	0.470	5.40	12.35	4.39	11.5	8.74	0.71	1.62	-3.61
C_3H_8	0.077	26.7	14.37	1.42	50.4	10.29	1.40	1.44	-4.08
C_2H_4	0.98	4.13	11.76	6.35	8.35	8.35	0.494	1.53	-3.41

Note: D_{25} and D_o in cm^2/sec; P_{25} and P_o in $\frac{cc\ (STP)\ cm}{cm^2\ sec\ cm\ Hg}$; k_{25} and k_o in $\frac{cc\ (STP)}{cc\ Atm}$;

E and ΔH in kcal/mole.

over a wide interval in 1/T. For an average temperature of 55°C (T = 323°), an uncertainty of 0.1 kcal in the heats results in an uncertainty of 15% in the preexponential factor.

Discussion

Permeation

In Table 3, the experimental permeation coefficients P_{25} at 25°C and the heats of permeation E_p of FEP (and PTFE) are compared with those of a linear and of a branched polyethylene PE Grex (Grace) and Alathon 14 (DuPont), 22% and 59% amorphous, respectively. The PE data are taken from Michaels and Bixler.[9] N_2 and O_2 permeate faster through the polyfluorocarbons than even through the low density PE. However, the relative rates shift in favor of PE with increasing boiling temperature (or with increasing molecular size) of the reactant.

In the following discussion of the two basic processes, solubility and diffusion, which together control permeation, only the data for linear PE (Grex) are used for comparison, since the degree of crystallinity of this PE does not change with temperature. We postulate that the crystallinity of the high-melting FEP, after annealing at 95°C, is constant also.

Solubility

The solubilities of gases in some nonpolar solvents at 25°C and atmospheric pressure have been found to be an exponential function of the Lennard-Jones force constant ε/k,[10] or the boiling temperature T_b.[11] The same functional relationship has been observed for the solubilities of gases in PE,[9] natural rubber,[12] and polyethylene terephthalate.[13] The heat of solution in PE is a linear function of ε/k also.[9] Since both ε/k and T_b are measures for the van der Waals' interaction forces of gases and differ only by an approximately constant factor, the discussion will be limited to ε/k.

In Fig. 3 the logarithms of the observed gas solubilities k_{25} at 25°C, and in Fig. 4 the heats of solution ΔH_S, are plotted versus ε/k for FEP. The values of ε/k are those given by Michaels and Bixler,[9] except that

Table 3

PERMEATION DATA FOR DIVERSE GASES IN PE, FEP, AND PTFE

Gas	$P_{25} \times 10^8$				E_P			
	PE (22)[1]	PE (59)[2]	FEP	PTFE[3]	PE (22)[1]	PE (59)[2]	FEP	PTFE[3]
N_2	0.11	0.74	1.2	1.1	9.5	11.8	7.3	5.8
O_2	0.31	2.2	3.7	3.2	8.4	10.2	6.1	4.5
CO_2	1.29	9.6	9.7	8.9	7.2	9.3	5.0	3.3
CH_4	0.36	2.2	0.66	---	9.7	11.3	8.3	---
C_2H_6	0.45	5.2	0.33	---	10.2	11.3	8.7	---
C_3H_8	0.44	7.2	0.11	---	9.3	11.2	10.3	---
C_2H_4	---	---	0.48	---	---	---	8.4	---

Note: P_{25} in $\frac{\text{cc (STP) cm}}{\text{cm}^2 \text{ sec atm}}$; E_P in kcal/mole.

[1] PE Grex, 22% crystalline, Ref. 9.
[2] PE Alathon 14, 59% crystalline, Ref. 9.
[3] PTFE, 60% crystalline, Ref. 1.

for C_2H_4, which is taken from Hildebrand et al.[10] The fit to straight lines is excellent (except for CO_2 which possibly interacts with FEP), but may be somewhat fortuitous since the values of the force constant ϵ/k are not quite certain.[11] The equations of the straight lines are

$$\log k_{25} = 1.38 + 0.0052\ \epsilon/k \tag{3}$$

$$\Delta H_S = -0.85 - 0.012\ \epsilon/k \text{ (kcal mole}^{-1}) \tag{4}$$

For PE the equivalent $\log k_{25}$ and ΔH_S plots have slopes of 0.0095 and 0.0164.[9]

The solubility k and the heat of solution ΔH_S are related by the expression

$$\log k = \log k_o - \frac{\Delta H_S}{2.3\ RT}$$

If k_o (or the standard entropy of solution, $\Delta S_o = 2.3 \log k_o/R$) of the different solutions were the same, the log k versus ΔH_S plot would be linear with a slope of $-1/2.3\ RT = -0.73$ kcal^{-1} mole at 298°K. The solubilities in PE satisfy this correlation.[9] For FEP (see Table 2) the k_o is, however, not constant; it is within the precision of measurements a linear function of ΔH_S (Fig 5) with a slope of -0.29 kcal-mole^{-1}.

The linear interdependence of the standard entropy and enthalpy of solution appears at least qualitatively plausible, since the higher heats of solution, i.e., stronger interactions, should be associated with reduced degree of freedom of the dissolved molecules.

A theoretical interpretation of the observed empirical correlations involving the Lennard-Jones force constant has been attempted by Michaels and Bixler.[9] It was based on the Hildebrand-Scatchard[14] model for the mixing of two liquids and that model's adaptation for polymers by Flory-Huggins.[15] In addition, the chemical potential of the gases was assumed to obey the simple Clausius-Clapeyron equation. A linear correlation between ΔH_S and ϵ/k was derived with a slope closely matching the experimental one, (0.0156 versus 0.0164 for PE).[9] This agreement between

observation and model is probably fortuitous because of the rather tenuous assumptions made for the model: (1) the Trouton rule holds, i.e., the entropy of vaporization at the boiling point is equal to 0.020 kcal/deg for all gases studied, (2) the (fictitious) heat of condensation is constant even above the critical point; and (3) the heat of mixing is always small relative to the heat of condensation, or is constant. Postulate (3), made implicitly, conflicts with the theory of mixing of liquids as formulated by Hildebrand and others[14] and with experimental data for such systems. The contradictions with theory are illustrated by the data summarized in Table 4. Indeed, for PE the heats of solution are by an approximately constant amount more positive than the heats of condensation; in contrast, for FEP the difference is negative for the low-boiling gases but decreases with increasing boiling point and becomes positive for propane. However, according to the simple theory of solution the heat of mixing can only be positive. Even larger negative heats of solution were found for gases in glassy polyethylene terephthalate;[13] they were ascribed to strong exothermic adsorption of the gases on the walls of internal voids.

The gas solubilities at 25°C are listed also in Table 4; for PE and PTFE they are corrected for crystallinity. The uncorrected solubilities in FEP which represent a lower limit are significantly higher than in PE for the low boiling gases; but the reverse holds for the higher boiling gases.

The solubilities of N_2, O_2, and CO_2 in PTFE appear to be significantly higher than in FEP, but the heats of solution are somewhat less negative. Both these differences may be explained by quasi-condensation of the gases in micropores of PTFE.

Diffusion

It is seen from Table 2 that the preexponential factor D_o (which is about proportional to the entropy of activation) varies significantly between solutes. In Fig. 6 the logarithm of D_o is plotted versus the activation energy of diffusion E_D of the gases in FEP. The data can be

Table 4

SOLUBILITY DATA FOR DIVERSE GASES IN PE, FEP, AND PTFE

Gas	ϵ/k	k_{25}			ΔH_S			
		PE[2]	FEP	PTFE[3]	Cond[4]	PE[2]	FEP	PTFE[3]
N_2	95	0.041	0.13	0.30	-1.33	0.5	-1.89	-1.30
O_2	118	0.077	0.21	0.52	-1.63	-0.4	-2.20	-1.73
CO_2	189	0.451	0.92	2.35	-3.46	-1.3	-3.75	-3.50
CH_4	148	0.203	0.22	--	-1.96	-0.7	-2.58	--
C_2H_6	243	1.28	0.71	--	-3.51	-2.3	-3.61	--
C_3H_8	284	3.97	1.40	--	-4.49	-3.0	-4.08	--
C_2H_4	200	--	0.49	--	-3.24	--	-3.41	--

Note: ϵ/k in °K; k_{25} in $\frac{cc(STP)}{cc\ atm}$; ΔH_S in kcal/mole.

[1] For PE and PTFE k_{25} is the solubility in amorphous phase; for FEP, k_{25} is the experimental solubility.
[2] Reference 9.
[3] Reference 1.
[4] Heat of condensation.

approximated by a linear relationship as has been observed also for other polymers.[16] A theoretical explanation has been given by Lawson.[17]

The activation energies and the diffusion constants at 25°C of PE, FEP, and PTFE are listed in Table 5. Rather surprisingly, the activation energies for the first two polymers are identical for all gases studied within the precision of the measurements. According to the model by Brandt and Anysas[18] the activation energy of diffusion has two components; one depends on the cohesive energy of the polymer and is proportional to the molecular diameter of the permeant, the other depends on the chain flexibility and is proportional to the square of the diameter. Michaels

Table 5

DIFFUSION DATA FOR DIVERSE GASES IN PE, FEP, AND PTFE

Gas	$D_{25} \times 10^7$			E_D		
	PE[1]	FEP	PTFE[1]	PE[1]	FEP	PTFE[1]
N_2	0.93	0.95	0.88	9.0	9.20	7.12
O_2	1.70	1.84	1.52	8.8	8.29	6.28
CO_2	1.24	1.05	1.03	8.5	8.75	6.84
CH_4	0.57	0.30	--	10.4	10.89	--
C_2H_6	0.146	0.047	--	12.5	12.35	--
C_3H_8	0.049	0.0077	--	13.6	14.37	--
C_2H_4	--	0.098	--	--	11.76	--

Note: D_{25} in $cm^2 sec$; E_D in kcal/mole.

[1] Reference 9.

and Bixler[9] estimate that for PE the contribution of the flexing energy to the activation energy is small, and accordingly find a linear relationship between the activation energies and the molecular diameters. In contrast, the cohesive energy of FEP is smaller than that of PE; but the FEP chain is stiffer. Therefore, the energy associated with chain flexing should be significant in FEP, and the activation energies of diffusion should increase more than linearly with the molecular diameter of the permeants.

Finally, a comparison between the activation energies of diffusion in FEP and PTFE (Table 5) is of considerable interest. Although the cohesive energy of PTFE is certainly quite similar to that of FEP and its chain stiffness is probably higher, the apparent activation energies for all the three gases studies is about 2 kcal lower. Thus, easier diffusion pathways must be available in the sintered PTFE; they very likely are

micropores and/or grain boundaries. According to the manufacturer, commercial PTFE has a void volume of about 0.5%; nevertheless, the density of PTFE increases by several percent if compressed at 4 kbar/inch^2.[19] Further study will be needed to show whether this increase is due to the removal of pores or to an increase in crystallinity.

Conclusions

Empirical correlations have been obtained in this and other studies between transport properties and molecular parameters of gases permeating through polymers. However, the apparently specific relationships observed for heat of solution and force constant, on the one hand, and activation energy of diffusion and molecular diameter on the other, may well be fortuitous. For the gases studied, the molecular diameters are approximately proportional to the Lennard-Jones force constants (or their boiling temperatures); thus, one could have used either of these parameters and still obtained linear correlations for the heats of solution or of diffusion. Hence, a plot of ΔH_S versus E_D for FEP is approximately linear also (Fig. 7); only CO_2 deviates again pronouncedly from the straight line.

In the short discussion of the data we have pointed out the inability of the existing theories of gas-polymer interactions to explain satisfactorily the experimental data for FEP and possibly for PE, also. It is beyond the scope of this present study to formulate models more consistent with the observations.

Finally, the conclusion that diffusion through PTFE proceeds at least in part along pores and grain boundaries may have a significance far beyond the diffusion process. Other observed properties of bulk PTFE, which have been ascribed to the dense polymer structure itself, may also be due in part to the physical structure of the sintered material. A reevaluation of PTFE properties on the basis of this model may well be worthwhile.

Acknowledgment

M. Christensen assisted in the experimental work, and F. J. Martinelli wrote the computer programs. This work was performed for the Jet Propulsion Laboratory, California Institute of Technology, sponsored by the National Aeronautics and Space Administration under Contract NAS 7-698.

REFERENCES

1. R. A. Pasternak, M. V. Christensen, and J. Heller, Macromol. 3, 366 (1970).

2. R. A. Pasternak, J. F. Schimscheimer, and J. Heller, J. Polymer Sci. 8, 467 (1970).

3. R. A. Pasternak and J. McNulty, Modern Packaging 43, 89 (1970).

4. R. A. Pasternak and M. V. Christensen, J. Appl. Phys., in preparation.

5. R. Kaiser, "Gas Phase Chromatography," Butterworths, London, 1963, p. 92.

6. C. W. Bunn and E. R. Howells, Nature 174, 549 (1954).

7. B. Heise, H. G. Killian, and F. H. Müller, Kolloid-Z. Z. Polym. 213, 12 (1966).

8. DuPont, Technical Information Bulletin T-2C.

9. A. S. Michaels and H. J. Bixler, J. Polymer Sci. 50, 393, 413 (1961).

10. J. E. Jolley and J. H. Hildebrand, J. Am. Chem. Soc. 80, 1050 (1958).

11. J. H. Hildebrand, Proc. Nat. Acad. Sci., U.S., 57, 542 (1967).

12. G. J. van Amerongen, Rubb. Chem. Technol. 37, 1065 (1964).

13. A. S. Michaels, W. R. Vieth, and J. A. Barrie, J. Appl. Phys. 34, 1, 13 (1963).

14. J. H. Hildebrand and R. L. Scott, "The Solubility of Non-Electrolytes," 3rd Ed., Reinhold Publishing Corp., New York, 1950.

15. P. J. Flory, "The Principles of Polymer Chemistry," Cornell Univ. Press, Ithaca, New York, 1953.

16. P. Meares, J. Am. Chem. Soc. 76, 3415 (1954), and Trans. Faraday Soc. 54, 40 (1957).

17. A. W. Lawson, J. Chem. Phys. 32, 131 (1960).

18. W. W. Brandt and G. A. Anysas, J. Appl. Polym. Sci. 7, 1919 (1963).

19. D. Lawson, private communication.

LEGENDS TO FIGURES

Fig. 1 Logarithm of the Permeation Coefficient P of Seven Gases in FEP, as a Function of the Reciprocal Temperature 1/T.

Fig. 2 Logarithm of the Diffusion Coefficient D of Seven Gases in FEP, as a Function of the Reciprocal Temperature 1/T.

Fig. 3 Logarithm of the Solubility k_{25} at 25°C of Seven Gases in FEP as a Function of the Lennard-Jones Force Constant ϵ/k.

Fig. 4 Heat of Solution ΔH_S of Seven Gases in FEP, As a Function of the Lennard-Jones Force Constant ϵ/k.

Fig. 5 Logarithm of the Preexponential Factor k_o of Seven Gases in FEP as a Function of Heat of Solution ΔH_S^o.

Fig. 6 Logarithm of the Preexponential Factor D_o of Seven Gases in FEP as a Function of Activation Energy of Diffusion E_D.

Fig. 7 Heat of Solution ΔH_S as a Function of Activation Energy of Diffusion E_D.

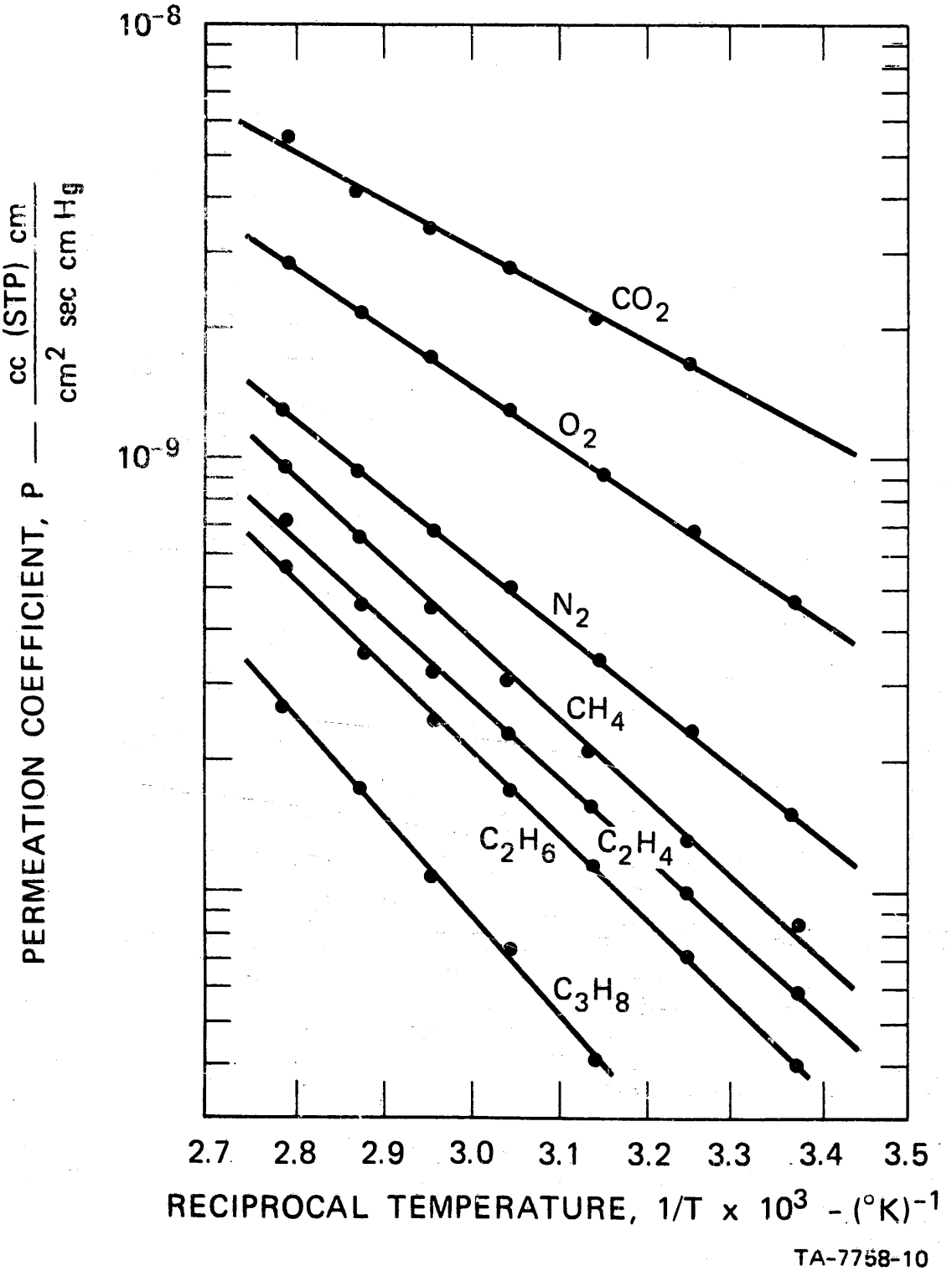

FIGURE 1

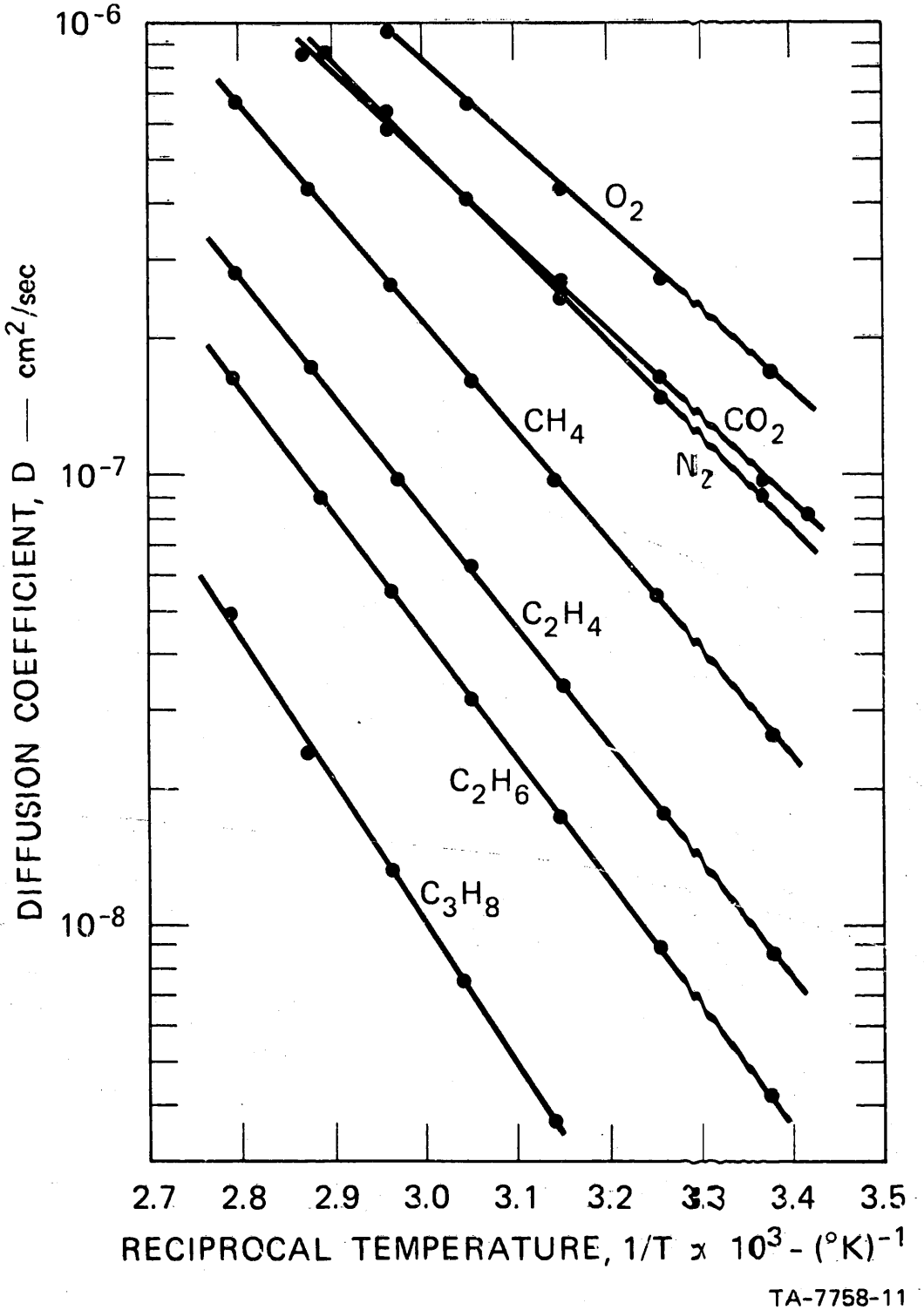
10^{-6}
10^{-7}
10^{-8}
DIFFUSION COEFFICIENT, D — cm^2/sec
O_2
CH_4
CO_2
N_2
C_2H_4
C_2H_6
C_3H_8
2.7
2.8
2.9
3.0
3.1
3.2
3.3
3.4
3.5
RECIPROCAL TEMPERATURE, $1/T \times 10^3 - (°K)^{-1}$
TA-7758-11

FIGURE 2

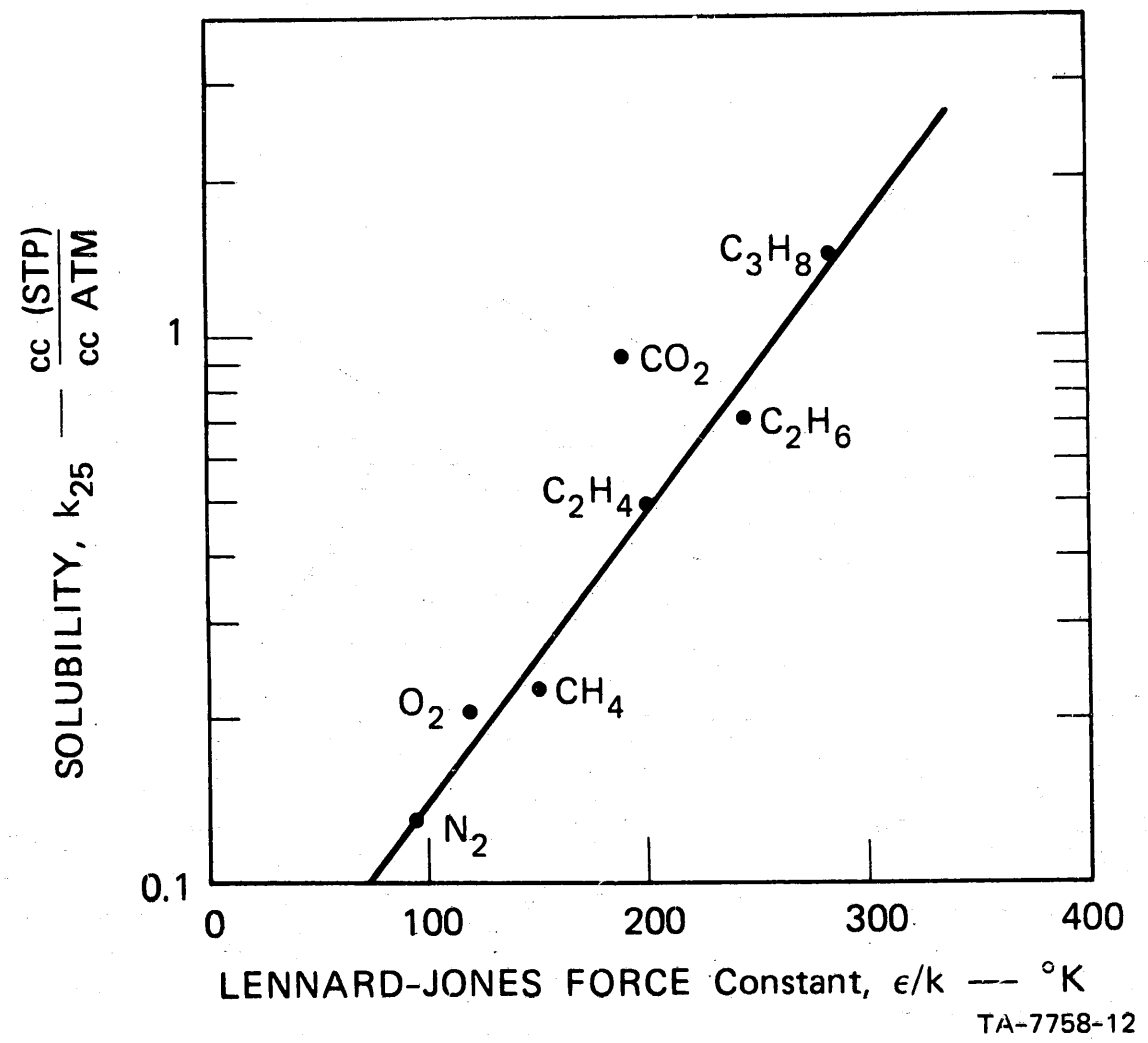
SOLUBILITY, k_{25} — $\frac{cc\ (STP)}{cc\ ATM}$
1
0.1
C_3H_8
CO_2
C_2H_6
C_2H_4
CH_4
O_2
N_2
0
100
200
300
400
LENNARD-JONES FORCE Constant, ϵ/k --- °K
TA-7758-12

FIGURE 3

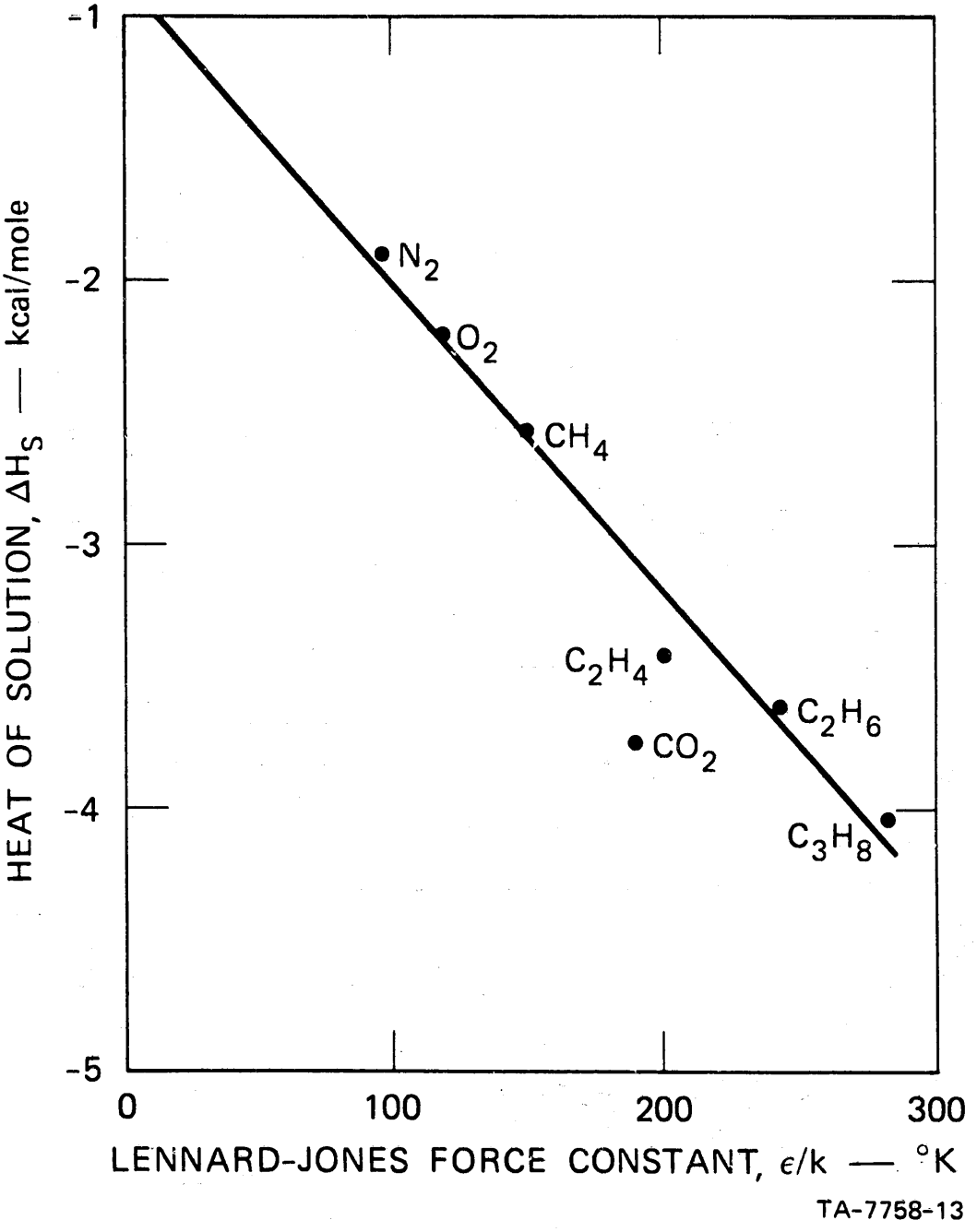
-1
-2
-3
-4
-5
HEAT OF SOLUTION, ΔH_S — kcal/mole
N_2
O_2
CH_4
C_2H_4
C_2H_6
CO_2
C_3H_8
0
100
200
300
LENNARD-JONES FORCE CONSTANT, ϵ/k — °K
TA-7758-13

FIGURE 1

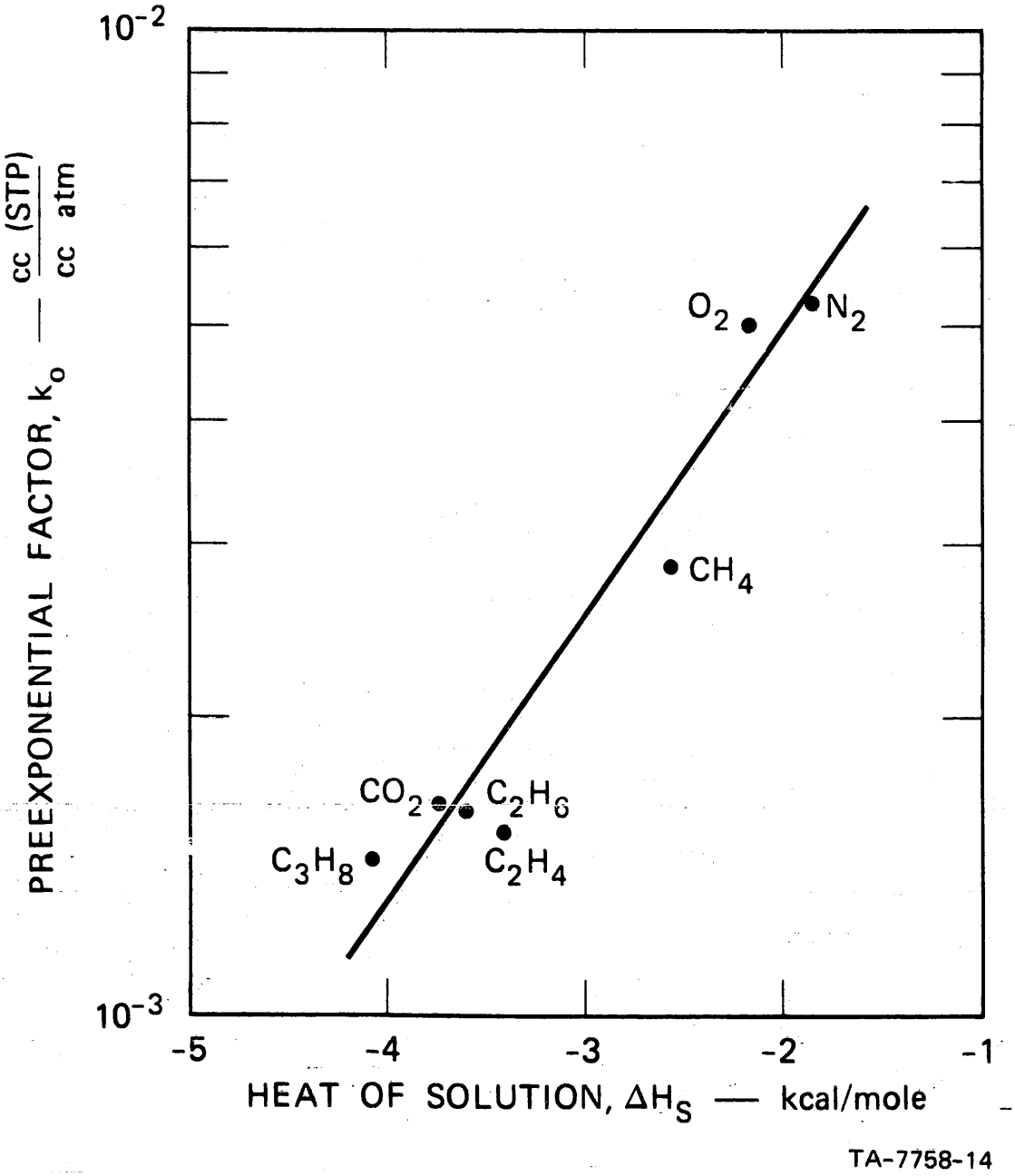
10^{-2}
10^{-3}
PREEXPONENTIAL FACTOR, k_o — $\frac{cc\ (STP)}{cc\ atm}$
O_2
N_2
CH_4
CO_2
C_2H_6
C_3H_8
C_2H_4
-5
-4
-3
-2
-1
HEAT OF SOLUTION, ΔH_S — kcal/mole
TA-7758-14

FIGURE 5

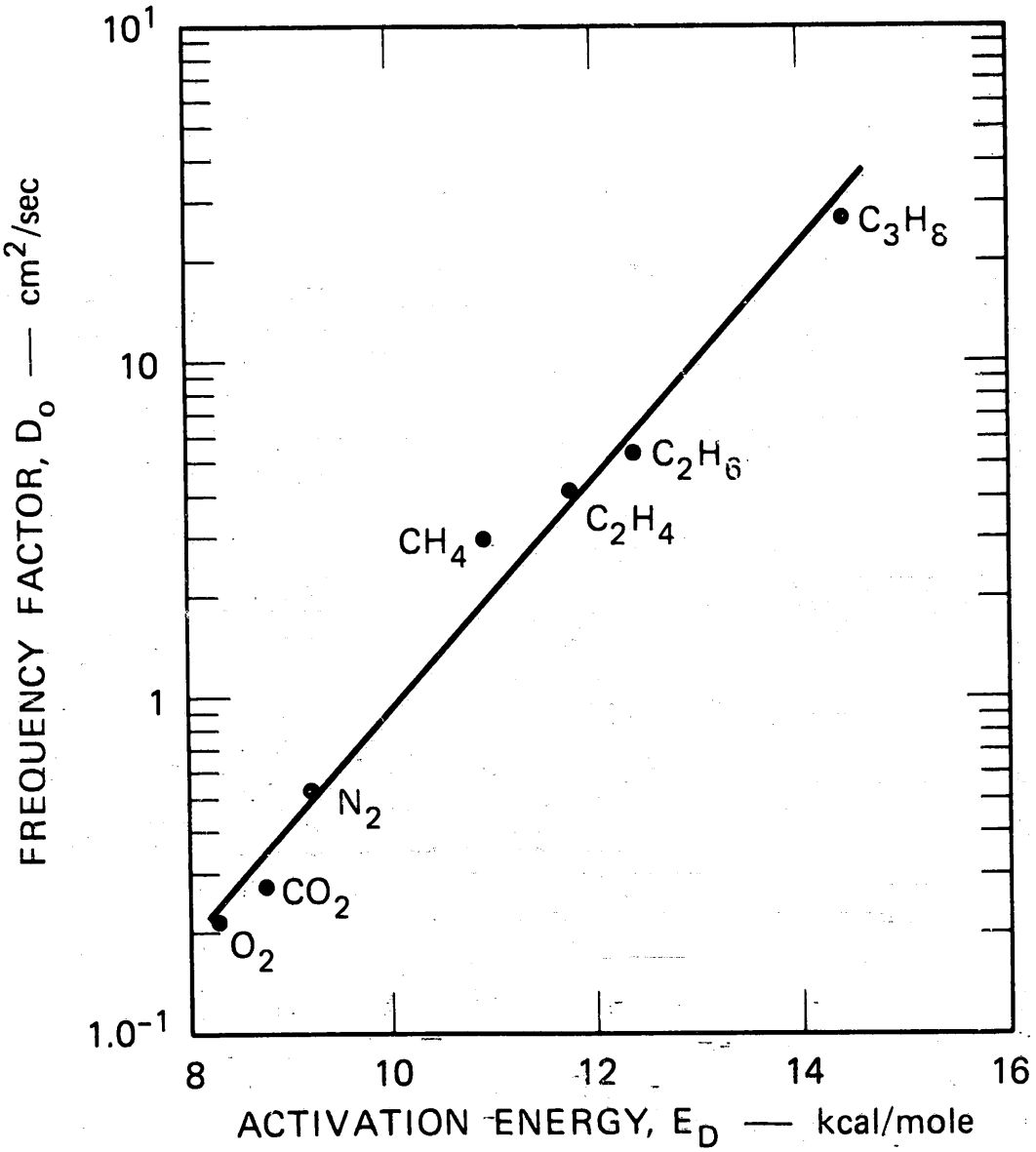
10^1
10
1
1.0^{-1}
FREQUENCY FACTOR, D_o — cm^2/sec
C_3H_8
C_2H_6
C_2H_4
CH_4
N_2
CO_2
O_2
8
10
12
14
16
ACTIVATION ENERGY, E_D — kcal/mole
TA-7758-15

FIGURE 6

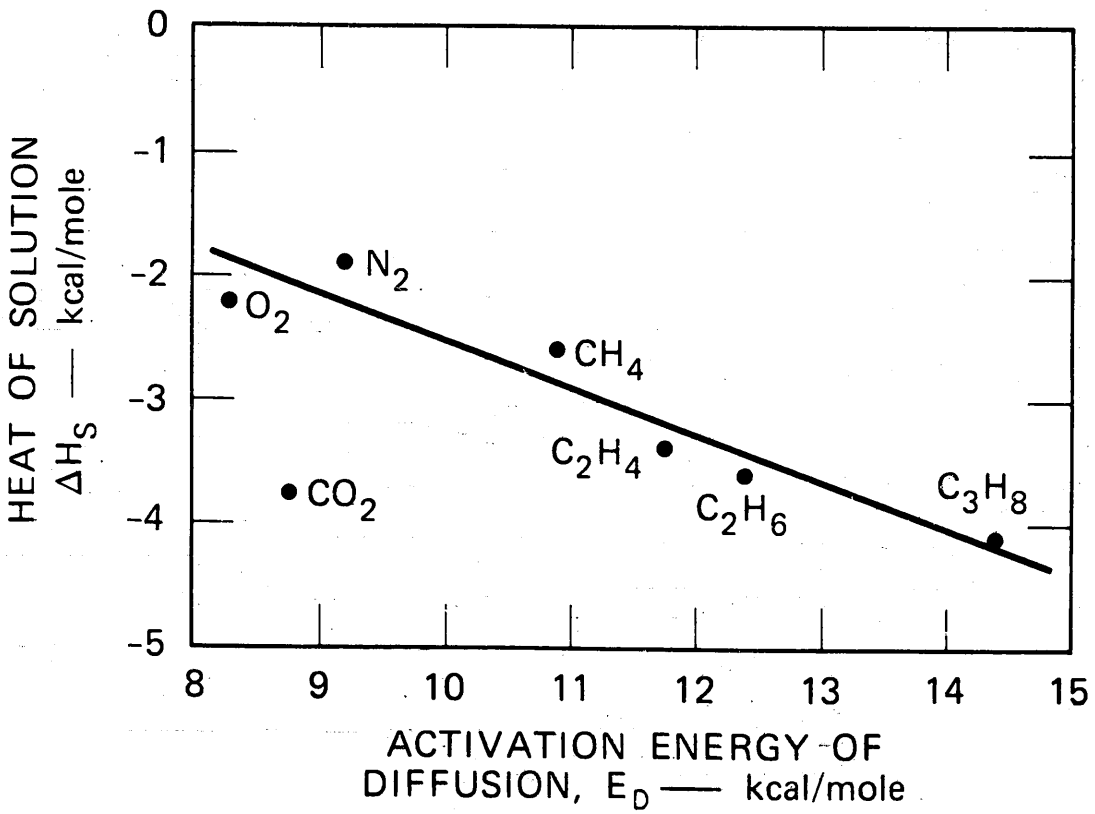

TA-7758-16

FIGURE 7

Appendix C*

VISCOUS FLOW AND DIFFUSION OF GASES THROUGH SMALL APERTURES

by

R. A. Pasternak and M. V. Christensen
Polymer Chemistry Program
Stanford Research Institute
Menlo Park, California 94025

ABSTRACT

In recent studies of diffusion and permeation of gases through polymer membranes,[1,2] the need was felt for a reliable method of determining detector sensitivities for a variety of gases. A simple calibration procedure has been devised; it is based on pressure controlled viscous flows of gases through small apertures. This concept has been elaborated by a systematic study of the mechanism of gas transport through apertures; the results of this work are reported here.

---

* To be published in J. Applied Physics.

Appendix C*

VISCOUS FLOW AND DIFFUSION OF GASES THROUGH SMALL APERTURES

by

R. A. Pasternak and M. V. Christensen
Polymer Chemistry Program
Stanford Research Institute
Menlo Park, California 94025

Experimental

The experimental unit, shown schematically in Figure 1, is basically the polymer Permeation Analyzer,* which is used for measuring transport of gases and vapors through polymer membranes,[3] except that the membrane is replaced by a pinhole or a capillary. A carrier gas at constant flow rate sweeps past the aperture to a detector, in the present design a katharometer. The test gas, which is either the pure tracer gas or its mixture with carrier gas, flows past the upstream side of the aperture; gas mixtures of known composition are prepared by adjusting the flow rates of the tracer and the carrier gases with needle valves (1 and 2) and measuring them individually with a soap bubble flow meter.

A pressure difference, Δp, which may be positive or negative (i.e., the pressure of the carrier gas is lower or higher than that of the test gas) is established across the aperture by throttling the two gas streams with needle valves (3 and 4) located at the exit ports; Δp is measured by a tube manometer, which is filled with a fluid of unit density. The precision in the manometer reading is about 0.5 mm. (The pressure difference is here expressed in mm of the unit-density fluid; thus, one mm is equal to 98.1 dynes/cm^2.)

* Manufactured by Dohrmann Instrument Co. (Infotronics), Mountain View, California.

In the present experiments, the carrier gas was helium, and the pressure in both gas streams was close to one atmosphere; the maximum pressure difference was less than 0.02 atmosphere. The temperature was maintained at about 25°C.

Tracer gas passes through the aperture by two mechanisms, diffusion and volume flow. The rate of transport F of the tracer gas is related to the observed detector signal S' by

$$F = k(f_o + V)S' \qquad (1)$$

where k is the sensitivity of the detector for the particular tracer gas, f_o is the flow rate of carrier gas, and V the volume flow of the test gas through the aperture. At high pressure differences, when viscous flow is the principal transport mechanism, the volume flow can be approximated by $V \approx F/c_o$, where c_o is the partial pressure of the tracer in the test gas.

Introduction of this expression into Eq. (1) leads to

$$(f_o + V) = f_o \left(\frac{1}{1 - \frac{kS'}{c_o}} \right) \qquad (2)$$

This correction to f_o amounted at most to about 3% in the present study.

The rate of transport can now be redefined by

$$F = kS$$

where $S = (f_o + V)S'$ is the signal normalized for an effective carrier gas flow rate of unity.

Finally, it was established by variation in the flow rate f_o that the detector response was linear with concentration over the range studied.

Theoretical

A. Derivation of Equation for Total Flow of Tracer Gas Through Aperture

Dilution and viscous flow occur simultaneously through the aperture, and their relative importance depends on pressure. One-dimensional total flow of tracer gas can be described by the differential equation[4]

$$\frac{dc}{dt} = D\frac{\partial^2 c}{\partial X^2} - u\frac{\partial c}{\partial X} \qquad (3a)$$

where c is the partial pressure of tracer gas at any point X in the flow channel, t is the time, D the diffusion coefficient, and u the linear, convectional flow rate of the test gas caused by external forces, here by a pressure gradient.

At steady state, Eq. (3a) reduces to

$$D\frac{\partial^2 c}{DX^2} - u\frac{\partial c}{dX} = 0 \qquad (3b)$$

The boundary conditions in our experiments are

$$c = c_o \quad \text{at } X = 0$$
$$c \approx 0 \quad \text{at } X = \ell$$

Now, c_o is the partial pressure of the tracer in the test gas, and ℓ is the length of the channel. Integration (at constant pressure difference) between the limits given and rearrangement results in the expression for the rate of transport F of the tracer gas through the aperture

$$F = \frac{(\pi r^2)\, uc_o}{1-\exp(-\frac{u\ell}{D})} \qquad (4a)$$

where πr^2 is the cross-sectional area of a cylindrical channel. In this integration, u and D are average values for a particular configuration and are assumed to be independent of X and c. However, u is a function of the pressure difference Δp; it can be positive or negative; in contrast, D should be independent of Δp, at least for the dilute gas mixtures, and should represent the interdiffusion coefficient of the tracer gas in the carrier gas.

At $\Delta p = 0$, the flow velocity u is zero, and Eq. (4a) reduces to the simple diffusion rate law

$$F_o = kS_o = \frac{\pi r^2 D c_o}{\ell} \tag{4b}$$

Introduction of F_o and $y = u\ell/D$ into Eq. (4a) leads to

$$\frac{F}{F_o} = \frac{S}{S_0} = \frac{1}{1-\exp(-y)} \tag{4c}$$

For large positive values of y (say $y > 4$), equivalent to high Δp values, Eq. (4a) reduces to

$$F = kS = \pi r^2 u c_o \tag{4d}$$

The parameter y is the ratio of the transport rates of the tracer gas by convectional flow and by diffusion; thus, in the intermediate pressure range the flux depends on both flow mechanisms. The diffusion coefficient D can be determined from the signal at $\Delta p = 0$, and u can be evaluated as a function of Δp from the experimental data by means of Eq. (4c), and the value of D.

B. Convectional Flow

In the preceding section it has been shown how the flow velocity u through the aperture can be derived from the experimental data. Since the total pressure in the experiments is high, approximately one atmosphere,

the flow can be expected to be viscous; the flow rate should be related to the pressure difference Δp across a cylindrical aperture by the modified Poiseuille equation

$$\Delta p = \frac{8\eta\ell}{r^2} u + 1.14\ \rho\ u^2 \qquad (5)$$

where η is the viscosity and ρ the density of the gas, and r and ℓ are the radius and length of the aperture.

The second term is an end correction which takes into account that the flow will be fully developed only after a finite distance. The equation holds if this term is less than about half the first term. Moreover, additional conditions must be satisfied:[5]

(1) The fluid must be incompressible. Compressibility of the gas can be disregarded when the Mach number M (the ratio of flow and sound velocity) is smaller than one third.

(2) The flow must be laminar. This condition holds when the Reynolds number $R = r\rho u/\eta$ is smaller than 1,000.

(3) The fluid must be immobilized at the tube wall.

Substitution of $y = u\ell/D$ into Eq. (5) results in

$$\Delta p = \frac{8\eta\ell}{r^2}\frac{D}{\ell} \cdot y + 1.14\ \rho\ \left(\frac{D}{\ell}\right)^2 y^2 = \alpha y + \beta y^2 \qquad (6a)$$

For large values of y; i.e., at high pressure differences, the flow velocity can be expressed by Eq. (4d), and the experimental data should fit the equation

$$\Delta p = \frac{8\eta\ell}{r^2}\left(\frac{kS}{c_o \pi r^2}\right) + 1.14\ \rho\ \left(\frac{kS}{c_o \pi r^2}\right)^2 = aS + bS^2 \qquad (6b)$$

Results and Discussion

Two apertures were studied, a glass capillary and a pinhole in a metal foil.

A. Capillary

The capillary radius r measured microscopically was $3.9 \pm 0.1 \times 10^{-3}$ cm, and its length ℓ, measured with a micrometer, was 0.47 ± 0.005 cm.

In Figures 2 and 3 the detector signal S is plotted versus the pressure difference Δp across the capillary for pure CO_2, O_2, N_2, CH_4, C_2H_6, C_2H_4, and C_3H_8 as tracer gases. Runs (not shown graphically) were also made with mixtures of tracer gases and helium.

The data points for all series are described very well by straight lines over the entire range of observation. It thus appears that the linear term of the Poiseuille equation (6) applies; i.e., that the correction term for end effects and the contribution of diffusion are both negligible. The highest flow velocity u obtained in any of the experimental series was about 5×10^2 cm/sec; estimates show that at this velocity the two corrections are insignificant and that the other conditions for the validity of the Poiseuille equation are satisfied also. Thus, the slope of the experimental line can be expressed in terms of the coefficients in Eq. (6b).

$$\frac{dS}{d\Delta p} = \frac{c_o \pi r^4}{8 \ell \eta k} = \frac{A c_o}{\eta k} \qquad (7)$$

where A is a constant which can be calculated from the dimensions of the aperture.

Equation (7) can be used in two ways: If the viscosity of the fluid is known, the sensitivity of the detector can be derived; also the reverse, if the sensitivity is known, the viscosity can be calculated.

In Table I, column 2, the slopes obtained for the pure gases and for the gas mixtures studied are listed; they are expressed in mm/dynes cm^{-2}.

Table I

RELATIVE SENSITIVITY FACTORS OF KATHAROMETER FOR DIFFERENT GASES, AND VISCOSITIES OF GAS MIXTURES FLOWING THROUGH A CAPILLARY

Gas	%	$dS/d\Delta p$ (mm $dyne^{-1}$ cm^2)	η (μ poise)	k_o obs.	k_o lit[7]
CO_2	100	2.23			
	100	2.23	148	1.00	1.00
	100	2.25			
O_2	100	1.36			
	100	1.34	202	1.21	1.17
N_2	100	1.65	175	1.14	1.09
CH_4	100	2.28	109	1.32	1.33
C_2H_6	100	3.75			
	100	3.77	91	0.97	0.94
C_2H_4	100	3.33	101	0.98	0.98
C_3H_8	100	5.21	80	0.79	0.72
CO_2	17.0	1.68	196	--	--
	8.6	1.69	196	--	--
O_2	32.7	1.26	216	--	--
	20.4	1.27	214	--	--
	13.1	1.32	206	--	--
	9.1	1.34	203	--	--
	6.2	1.34	203	--	--
C_2H_6	42.2	3.26	105	--	--
	21.0	2.84	120	--	--
	14.8	2.59	132	--	--
	6.5	2.20	156	--	--

Note: The viscosities of the pure gases are taken from the literature:[6] those of the gas-helium mixtures are calculated from the experimental data.

Repeat runs are shown for three gases to indicate the reproducibility of the results. The viscosities for the pure gases are given in column 3; they are taken from the literature.[6] Column 4 shows the detector sensitivities k_o relative to that of CO_2, and in column 5 the relative sensitivities derived from a tabulation by Kaiser[7] are listed. The agreement between the two sets of data is quite satisfactory. Moreover, the detector sensitivites for CO_2, O_2, and N_2 were determined directly with gas mixtures of known composition. The relative values agreed with those given in column 4 within the precision of the measurements.

The absolute sensitivity of the detector can be calculated by means of Eq. (7) from the dimensions of the capillary. We obtain for CO_2

$$k_\eta = 4.82 \times 10^{-7} \text{ cc/mm}$$

the direct calibration with the CO_2-He gas mixture gave

$$k = 5.82 \times 10^{-7} \text{ cc/mm}$$

This agreement is quite acceptable. The estimated uncertainty in the radius of the capillary was about 2.5%, and thus the experimental uncertainty in k_η is at least 10%, since the radius enters with its fourth power. Moreover, the Poiseuille equation is derived for an idealized case and the deviation of 20% found here is easily possible for a real conductance.

In the lower half of Table I the data for gas mixtures are given. Here, the viscosities are calculated from the slopes and the sensitivity factors which were derived for the pure gases. Figure 4 is a graphical representation of the data. Obviously the viscosities must approach at infinite dilution that of pure helium (196μ poise); but we observe rather surprisingly different concentration effects for the three gases studied. However, dependence on composition similar to that for the He-O_2 mixtures has been reported for He-Ar mixtures.[8] A more extensive and thorough experimental and theoretical study of the viscosity of gas mixtures would be worthwhile.

B. Pinhole

The pinhole dimensions were $r = 5.0 \pm 0.2 \times 10^{-4}$ cm and $\ell = 4 \pm 1 \times 10^{-4}$ cm. They were measured microscopically, but the length determination required cross-sectioning of the foil.

The gases CO_2, O_2, and N_2 (pure and diluted with He) were studied both for positive and negative pressure differences.

The data were evaluated according to Eq. (4c); i.e., the parameter $y = u\ell/D$ was computed from the ratio S/S_o. A typical experimental run is shown in Figure 5 for a 22.2% CO_2-He mixture. The parameter y is also plotted in the figure; within the precision of the measurements it is a linear function of Δp over the entire range of observation. Linear correlations of the same quality were obtained for all gas mixtures. For the pure gases, significant deviations from linearity were observed. This linear dependence of y on Δp indicates that the flow velocity u obeys the one-term Poiseuille equation (5) with the viscosity independent of Δp, and that the diffusion coefficient D is constant also.

The maximum flow velocity in these experiments was about 2×10^3 cm/sec. Both the Mach and the Reynolds numbers are at this velocity small enough to satisfy the conditions for viscous flow. However, for the mixtures the square term in Eq. (5) was calculated at the highest velocities to be 10 to 20% of the linear term. The experimental results suggest that the second-order term is smaller than that estimated from the equation; or that it is compensated by other effects not considered here. Because of the high density of the pure gases, however, the second term should be so large that the Poiseuille equation must break down completely; still, approximately straight lines were obtained even for them, although the fit was less satisfactory.

The viscosity and the diffusion coefficient cannot be strictly constant over the whole pressure range studied, since the composition of the gas along the length of the aperture and its average must be a function of flow rate (or pressure difference). However, for the dilute gases, the concentration of the tracer being at most about 20%, the

variation in concentration will not be large. Moreover, the diffusion coefficients of gas mixtures have been shown to be barely dependent on composition,[9] and we have found the same for the viscosities of CO_2-He and O_2-He mixtures flowing through a capillary (see above). For pure gases, however, both parameters must vary significantly with pressure since the composition changes from one extreme to the other.

In Table II are shown the slopes of the y versus Δp plots, the diffusion coefficients derived from the signals at $\Delta p = 0$ by Eq. (4b), and the viscosities calculated from the slopes as defined by Eq. (6a)

$$\frac{dy}{d\Delta p} = \frac{r^2}{8} \cdot \frac{1}{D\eta} \tag{8}$$

The data for the pure gases are included also but are omitted from the discussion.

Table II

DIFFUSION AND VISCOSITY OF
GASES FLOWING THROUGH A 10-μ PINHOLE

Gas	%	$dy/d\Delta p$ (cm^2/dyne X 10^4)	D (cm^2/sec)	η (μ poise)
CO_2	100.0	7.75	0.123	328
	22.2	6.30	0.189	262
	16.0	6.30	0.189	262
	11.2	6.45	0.180	268
O_2	100.0	5.25	0.158	376
	20.2	4.82	0.228	254
	10.8	4.98	0.258	243
N_2	100.0	5.86	0.163	326
	21.6	5.25	0.228	260
	18.3	5.39	0.226	256
	10.6	5.37	0.250	232
	9.1	5.40	0.252	229

The experimental uncertainties affect the parameters given in Table II to a varying extent. The slopes $dy/d\Delta p$ are obtained from the measured signal and pressure difference only and are therefore quite reliable. Table II shows that for a given tracer gas the slopes; and therefore the products ηD are approximately independent of the composition of the gas mixture. Thus, both η and D must be constant for a given tracer gas, as suggested already; the alternative explanation that they are inversely proportional to each other is excluded since they are both similarly related to the cross sections of the gas molecules.

The calculation of the diffusion coefficients involves the square of the radius and the length of the aperture; these parameters are associated with large experimental errors but are in common for all experimental series. However, the specific test gas composition, the measurement of which is not of highest precision, enters individually into each run. Therefore, the variation of D with composition is probably associated primarily with this experimental uncertainty.

Finally the viscosity, by its mode of calculation, includes all the uncertainties associated with the diffusion coefficient. The pinhole radius enters, however, with its fourth power into the calculations.

In Table III the average observed diffusion coefficients and viscosities are compared with the interdiffusion coefficients calculated by the Stefan-Maxwell[10] formula, which usually agrees well with experimental data, and with the viscosity of helium taken from the literature.

The observed values of D are smaller than the calculated ones by approximately a constant factor. This observed reduction in D is far too large to be explained by the experimental errors in the measurements of the pinhole dimensions but appears to be real; the diameter and length of the pinhole are of the same magnitude, and thus diffusional flow is impeded by collision of the molecules with the walls.

The viscosity of the dilute gases can be expected to approach that of pure He, irrespective of the tracer gas. We find approximately the same viscosity for the three dilute gases studied. The agreement with the

Table III

COMPARISON OF OBSERVED, AVERAGED, AND CALCULATED DIFFUSION COEFFICIENTS AND VISCOSITIES OF DILUTE GASES IN HELIUM, PINHOLE DATA

Gas	D (cm^2/sec)		D_{obs}/D_{calc}	η (μ poise)	
	obs	calc		obs	He
CO_2	0.185	0.44	0.42	264	
O_2	0.24	0.62	0.29	264	197
N_2	0.24	0.59	0.41	245	

literature value for He is surprisingly close; the fourth power of the radius and the first power of the length of the aperture, both parameters being measured with low precision, enter into the calculation of the experimental value.

Acknowledgment

The authors are indebted to David Wooten for his help in the mathematical analysis of the flow problem and to R. Martinelli for writing the computer programs. This research was supported in part by the Jet Propulsion Laboratory, California Institute of Technology, sponsored by the National Aeronautics and Space Administration under Contract NAS 7-698.

REFERENCES

1. R.A. Pasternak, J. F. Schimscheimer, and J. Heller, J. Polymer Sci. 8, 467 (1970).

2. R. A. Pasternak, M. V. Christensen, and J. Heller, Macromol. 3, 366 (1970).

3. R. A. Pasternak and J. A. McNulty, Modern Packaging 43 89 (1970).

4. W. Jost, "Diffusion in Solids, Liquids, Gases," Academic Press, New York, 1952, p 46.

5. S. Dushman, "Scientific Foundations of Vacuum Technique," 2nd Ed., John Wiley and Sons, New York, 1962, pp 83-85.

6. "Handbook of Chemistry and Physics," 47th Ed., Chemical Rubber Publishing Company, Cleveland, Ohio, F 39.

7. R. Kaiser, "Gas Phase Chromatography," Butterworths, London, 1963, p 92.

8. E. H. Kennard, "Kinetic Theory of Gases," McGraw-Hill Book Co., New York, 1938, p 162.

9. E. H. Kennard, ibid, p 197.

10. E. H. Kennard, ibid, p 193.

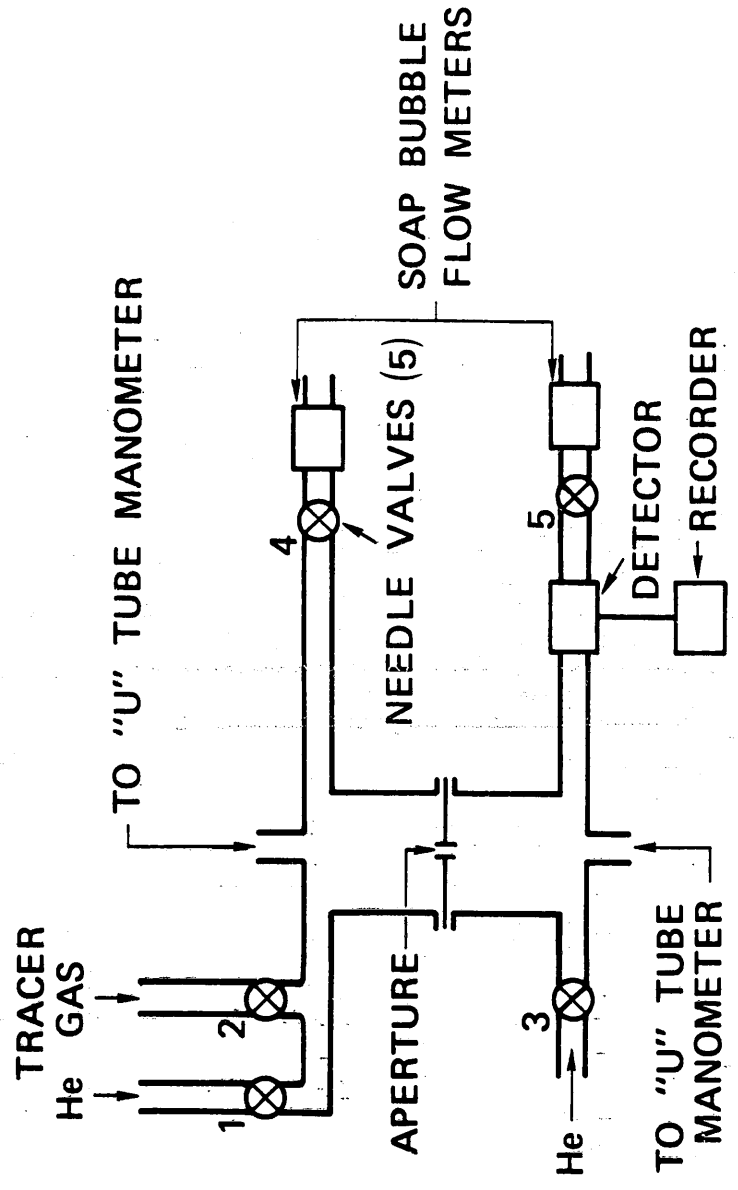

TA-7758-17

FIGURE 1 SCHEMATIC DRAWING OF FLOW SYSTEM

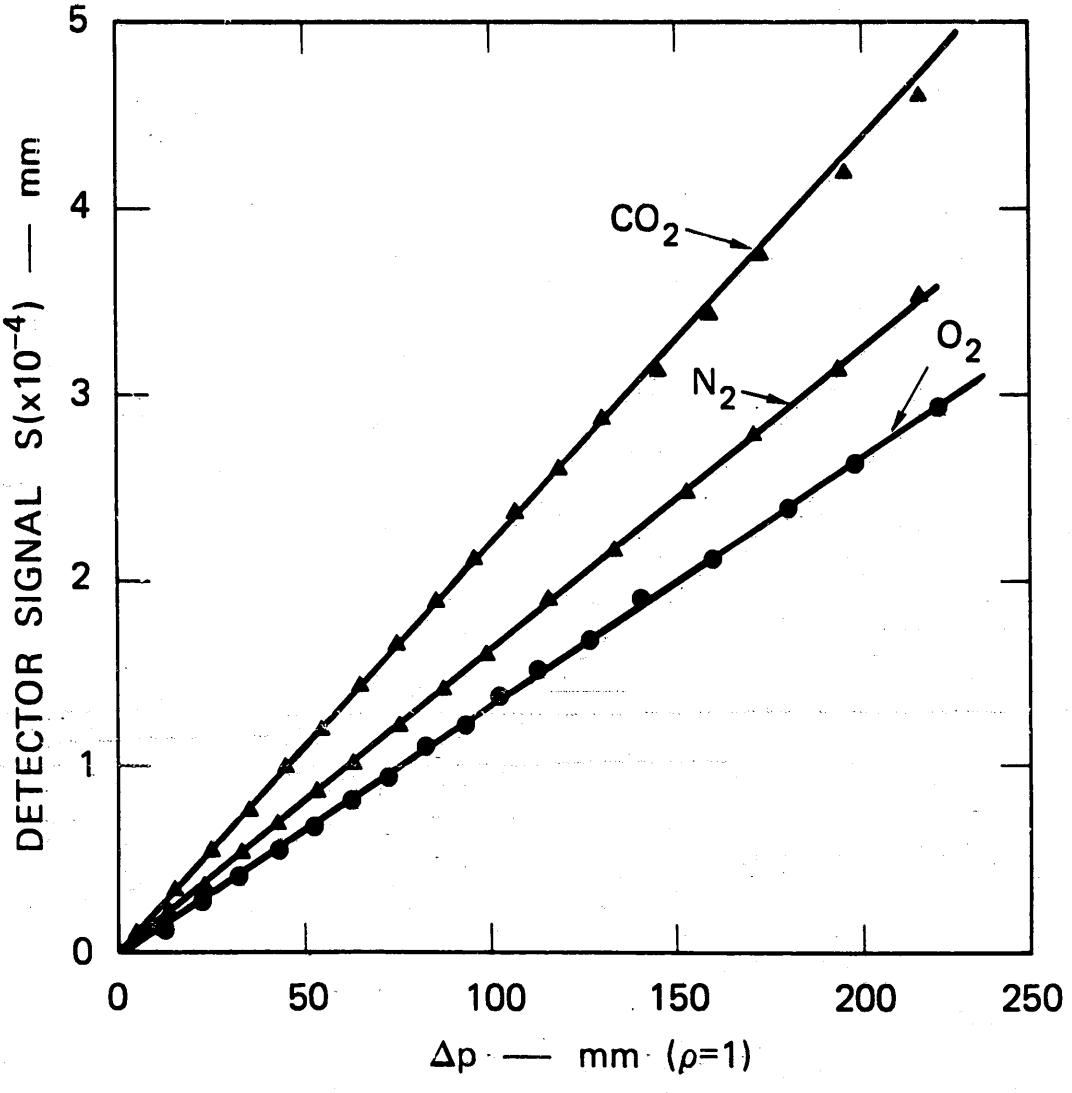

FIGURE 2 DETECTOR SIGNAL S VERSUS PRESSURE DIFFERENCE ΔP FOR CO_2, N_2, AND O_2. Data taken with capillary.

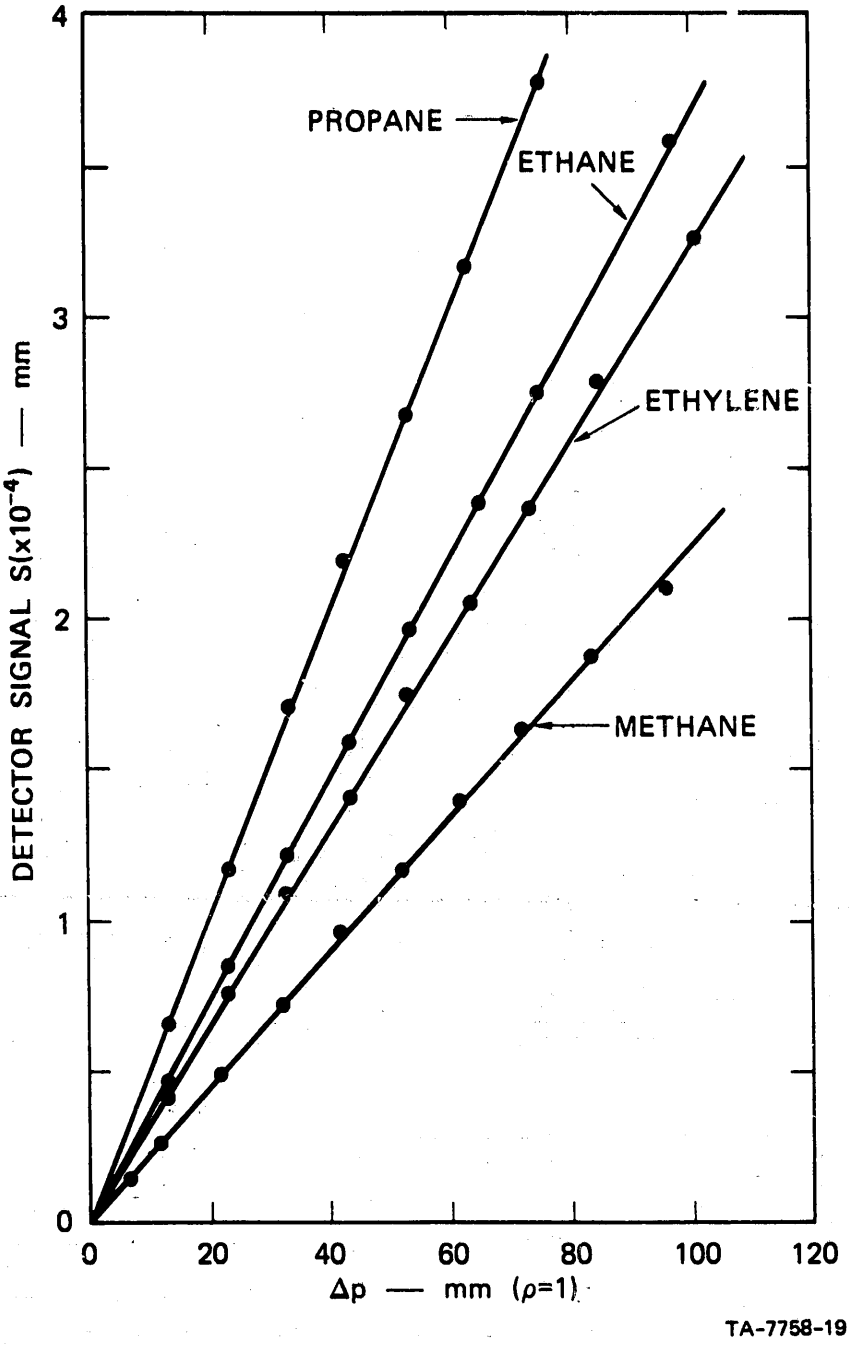

FIGURE 3 DETECTOR SIGNAL S VERSUS PRESSURE DIFFERENCE ΔP FOR PROPANE, ETHANE, ETHYLENE, AND METHANE. Data taken with capillary.

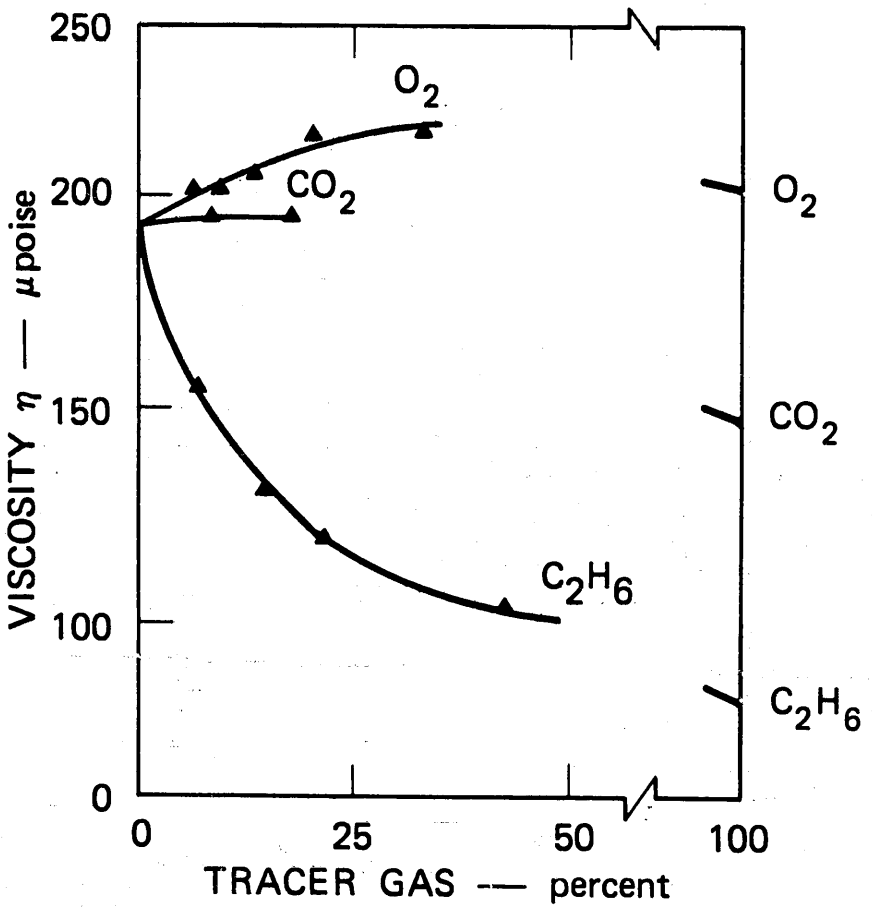

TA-7758-20

FIGURE 4 VISCOSITIES OF HELIUM-TRACER GAS MIXTURES AS A FUNCTION OF COMPOSITION. Data taken with capillary.

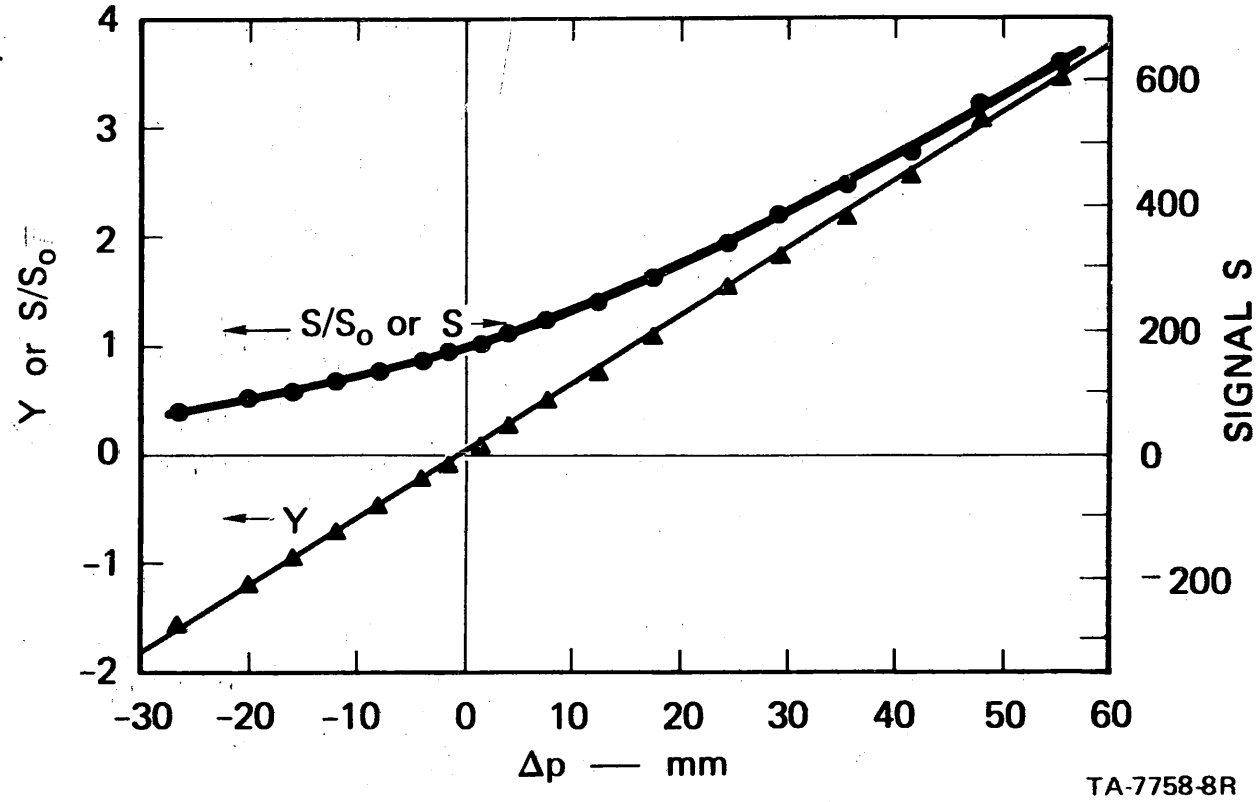

FIGURE 5 RELATIVE SIGNAL S/S_o (OR SIGNAL S) AND $Y\ (= \frac{\mu\ell}{D})$ VERSUS PRESSURE DIFFERENCE ΔP. Data taken with pinhole.

Appendix D*

DIFFUSION AND PERMEATION OF GASES THROUGH NITROSO RUBBER

by

R. A. Pasternak and M. V. Christensen
Polymer Chemistry Program
Stanford Research Institute
Menlo Park, California 94025

ABSTRACT

Nitroso rubber is of considerable interest for air space applications because of its resistance to strong oxidants and its good low-temperature flexibility.[1] A limited study of transport gases through this rubber has been carried out since such information is of importance for its potential use.

* To be published in J. Applied Polymer Science.

Appendix D

DIFFUSION AND PERMEATION OF GASES THROUGH NITROSO RUBBER

by

R. A. Pasternak and M. V. Christensen
Polymer Chemistry Program
Stanford Research Institute
Menlo Park, California 94025

Experimental

Two nitroso rubber samples were studied. One sample membrane had been manufactured by Thiokol Chemical Corp. (CTVR-CTA cured); its thickness was 35.0 ± 0.5 mil. The second sample was prepared in our laboratory from materials procured by Mr. D. Lawson from Jet Propulsion Laboratory, Pasadena. Nitroso terpolymer (100 parts), Cab-O-Sil silica (20 parts), and chromium trifluoroacetate (5 parts) were blended by standard procedures and cured at 307°F for 45 minutes; the resulting membrane had a thickness of 20 ± 3 mil. Both membranes were very soft and elastic.

High purity (99%+) O_2, N_2, CO_2, CH_4, C_2H_6, and C_3H_8 from cylinders were used without drying.

The instrument and the methods for measuring diffusion and permeation coefficients have been described elsewhere.[2,3] Determinations were made at about 60, 70, 80, and 90°C; for these thick membranes, the transmission rates became too small at lower temperatures to permit reliable measurements.

In Table I the permeation and diffusion coefficients P and D at 60°C, and the heats of permeation and diffusion E_P and E_D are tabulated. Since at most four experimental points were available for each Arrhenius plot (and only three for the thicker Thiokol membrane), the uncertainties in the heats, which are proportional to the slopes, are quite large, possibly 0.5 kcal/mole. The solubilities k, which are included in the table, are derived from the permeation and diffusion data in the usual way, $k = P/D$.

Table I

TRANSPORT DATA FOR NITROSO RUBBER

(a) SRI Membrane

Gas	$P_{60} \times 10^8$	E_P	$D_{60} \times 10^6$	E_D	$k_{60} \times 10^2$	ΔH_S
N_2	1.05	7.1	3.2	6.9	0.33	0.2
O_2	2.1	5.3	4.3	6.3	0.49	-0.1
CO_2	4.8	5.2	1.2	8.8	4.0	-3.5
CH_4	1.15	6.7	2.6	7.5	0.44	-0.8
C_2H_6	1.30	6.5	1.0	8.3	1.3	-1.8
C_3H_8	1.35	5.9	0.56	8.7	2.4	-2.8

(b) Thiokol Membrane

Gas	$P_{60} \times 10^8$	E_P	$D_{60} \times 10^6$	E_D
O_2	2.0	5.6	5.4	5.7
CO_2	4.6	4.9	1.6	8.2
C_2H_6	1.3	6.3	1.3	7.9

Note: P in $\frac{\text{cc (STP) cm}}{\text{cm}^2 \text{ sec cm Hg}}$, D in cm^2/sec, k in $\frac{\text{cc (STP)}}{\text{cc cm Hg}}$

E_P, D_D, and ΔH_S in kcal/mole.

The data obtained for the two membranes agree quite closely, if one takes into account the rather large uncertainties in the measurements.

The transport parameters follow a systematic pattern. The diffusion coefficients decrease and the solubilities increase with increasing boiling point (or molecular diameter) of the gases; the inverse holds for the heats of diffusion and solution. Similar correlations have been found for polyethylene[4] and FEP teflon.[5]

The transport properties of N_2, O_2, CO_2, and CH_4 in nitroso rubber (extrapolated to 25°C) and in natural rubber,[6,7] are compared in Table II The diffusion coefficients and the activation energies of diffusion of the gases (except of CO) are about the same in the two rubbers, but the solubilities are 2 to 4 times larger in the nitroso rubber, which is therefore more permeable. The somewhat different pattern for CO_2 may indicate strong specific interactions between CO_2 and the nitroso rubber.

Table II

COMPARISON BETWEEN NITROSO (Ni) AND NATURAL (Na) RUBBER

Gas	$D_{25} \times 10^6$		E_D		k_{25}		$P_{25} \times 10^7$	
	Ni	Na	Ni	Na	Ni	Na	Ni	Na
N_2	0.92	1.1	6.9	8.7	0.23	0.005	2.1	0.6
O_2	1.35	1.6	6.3	8.3	0.46	0.112	6.2	1.8
CO_2	0.25	1.1	8.8	8.9	5.8	0.90	14.5	9.9
CH_4	0.66	0.1	7.5	8.7	0.43	0.25	2.8	2.2

Note: D in cm^2/sec, k in $\frac{cc\ (STP)}{cc\ atm}$, P in $\frac{cc\ (STP)\ cm}{cm^2\ sec\ atm}$,

E_D in kcal/mole.

Acknowledgement

The authors are indebted to Mr. David D. Lawson for suggesting this research and for furnishing the materials. The work was supported by the Jet Propulsion Laboratory, California Institute of Technology, Pasadena, California, sponsored by the National Aeronautics and Space Administration under Contract NAS 7-698.

REFERENCES

1. N. B. Levine, Applied Polymer Sym. 11, 135 (1969).

2. R. A. Pasternak, J. F. Schimscheimer, and J. Heller, J. Polymer Sci. 8, 467 (1970).

3. R. A. Pasternak and J. McNulty, Modern Packaging 43, 89 (1970).

4. A. S. Michaels and H. J. Bixler, J. Polymer Sci. 50, 373, 413 (1961).

5. R. A. Pasternak, M. V. Christensen, and J. Heller, Macromol 3, 366 (1970).

6. G. J. van Amerongen, Rubb. Chem. Technol. 37, 1101 (1964).

7. "Diffusion in Polymers," Ed. by J. Crank and G. S. Park, Academic Press, London, 1968, p 50.

Appendix E

Besides the four papers accepted for publication as a result of work on this project, the following papers incorporate some information generated under this program or under a related NASA-JPL program.

1. A Dynamic Approach to Diffusion and Permeation Measurements by R. A. Pasternak, J. F. Schimscheimer, and J. Heller, Polymer Preprints 10, (2) 1234 (1969). This paper was presented at the 1969 New York meeting of the ACS.

2. A Dynamic Approach to Diffusion and Permeation Measurements by R. A. Pasternak, J. F. Schimscheimer, and J. Heller, J. Polymer Sci. A2, May 1970.

3. Measuring Transmission Rates of Gases, Vapors, and Liquids Through Plastics by R. A. Pasternak and James A. McNulty, Modern Packaging Magazine, April 1970.

4. Performance and Some Novel Applications of the Polymer Permeation Analyzer by R. A. Pasternak, G. L. Burns, and J. A. McNulty, paper presented at the Pittsburgh Conference on Analytical Chemistry and Applied Spectroscopy, Inc., March 1-6, 1970.